Universitetet i Stavanger

FACULTY OF SCIENCE AND TECHNOLOGY

BACHELOR'S THESIS

Studieprogram:	Semester:
Maskiningeniør	Spring/ Autumn semester, 2021
Author: Sondre Andersen Gysland Kjell Vistnes Randeberg	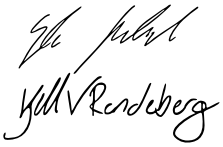

Programme coordinator: Knut Erik Teigen Giljarhus

Supervisors: Knut Erik Teigen Giljarhus, Jørgen Apeland

Title of bachelor 's thesis:

Improvement of efficiency of a coaxial octodrone

Credits: 20

Keywords: Coaxial, Blade element momentum theory, pyBEMT, propeller diameter, propeller spacing, pitch, flight time.	**Number of pages:** 64 Stavanger, 14/05/2021

Faculty of Science and Technology

Summary

The goal of this thesis is to find the optimal coaxial configuration for Nordic Unmanned´s drone Staaker BG200. Research has shown that the parameters propeller spacing and diameter, are factors that have the greatest impact on efficiency, as well as being parameters that can be optimized on the Staaker BG200. This thesis aims to improve the efficiency of a coaxial unmanned aerial vehicle and consequently extending the flight time. This will be achieved by a theory that describes the interaction between the propellers and analysis of experimental data.

Based on the literature study, testing hovering performance and communication with Nordic Unmanned the test plan was developed. Testing of every configuration of 28", 30" and 32" propeller was completed, with five different distances. The tests were performed on a test rig at UiS, which is capable of measuring a number of variables including thrust and power. Every test was driven by a test script that started the propellers at 24 Newtons of thrust, take sixteen steps, ending at 99 Newtons and record data points at every stop to a CSV-file.

Analyzing the results from the CSV-file, the result indicate that the configuration Nordic Unmanned are using today, with two 28" propellers, is not efficient compared to larger propeller sizes. However, the spacing between the propellers is sufficient.

Through analysing the results, Nordic Unmanned may improve their flight time with about 10 % or 2.6 minutes extra flight time if they change Staaker BG200s propeller from two 28" propellers to two 30" propellers, with the distance of 109.2 mm which they are using today. Further research using a more powerful motor is needed to see if the efficiency of the 32" propeller changes. Tests should also be performed in a wind tunnel to see the influence of forward flight.

Preface

Finishing our Mechanical engineering degree at the University of Stavanger, has been a delight because of Nordic Unmanneds suggested problem proposal. First of all, we would like to thank our supervisor from UiS Dr. Knut Erik T. Giljarhus, for guiding us with the theoretical model, the literature study and letting us use his pyBemt python script. Secondly, we would like to thank our supervisor at Nordic Unmanned, Jørgen Apeland, that guided us by giving us practical insight in unmanned aerial vehicle technology, setting up the test rig and helping us with the articles to use in the literature study. Thirdly, we would like to thank workshop engineer Jørgen Grønsund for sharing his practical experience, helping us with practical problems and setting up the test rig. And last but not least, we would like to thank the University of Stavanger for providing us with a good education and for letting us use their facilities.

Contents

1 Introduction **1**
1.1 Scope . . . 2
1.1.1 Learning objectives . . . 2
1.1.2 Performance targets . . . 2
1.1.3 Limitations . . . 2

2 Literature study **4**
2.1 Propeller configurations . . . 6
2.2 Propeller spacing . . . 7

3 STAAKER BG-200 **9**

4 Theory **10**
4.1 Simple momentum theory . . . 10
4.2 The blade element theory . . . 16
4.3 The blade element momentum theory . . . 19
4.4 Coaxial setup . . . 22
4.5 Efficiency . . . 25

5 Geometric description of propeller **26**
5.1 3D-Scanning . . . 26
5.2 Cutting of propeller . . . 29
5.3 Pybemt . . . 31
5.4 Optimising propeller . . . 32

6 Experimental setup **33**
6.1 HMS . . . 33
6.2 Test setup . . . 34
6.2.1 Motors . . . 36
6.2.2 propellers . . . 37
6.2.3 Tachometer . . . 37
6.2.4 Load cell . . . 38
6.2.5 Power supply . . . 38
6.3 RCbenchmark Script . . . 39
6.4 Test plan . . . 40

7 Results **43**
7.1 Calibration test . . . 43
7.2 BEMT . . . 44
7.3 Propeller spacing . . . 46
7.4 Propeller configuration . . . 50
7.5 Optimizing the propeller . . . 53

8 Discussion **55**
8.1 Propeller spacing 55
8.2 Propeller configuration 57
8.3 Flight time 58
8.4 Possible sources of error: 59
8.5 Future work 61
8.6 Recommendations 61

9 Conclusion **62**

References **63**

Appendix **65**

A Example python script for reading CSV-file **66**

B Example python script importing and plotting data **71**

C RCbenchmark script **75**

List of Figures

2.1 Affected area . . . 7
2.2 Propeller spacing . . . 8
3.1 Staaker BG200 . . . 9
4.1 Actuator disc model . . . 11
4.2 Wind velocity vectors . . . 15
4.3 Blade section . . . 16
4.4 Loads acting on airfoil . . . 17
5.1 BEMT input requirements . . . 26
5.2 3D-Scan . . . 27
5.3 3D scanned mesh of propeller . . . 28
5.4 Zoomed in 3D scanned mesh . . . 28
5.5 3D sections . . . 29
5.6 Propeller cutting . . . 30
5.7 Comparison airfoil section . . . 31
5.8 Wind velocity vectors including exhaust particles . . . 32
6.1 RcBenchmark series 1780 . . . 34
6.2 Test setup . . . 35
6.3 T-motor U8II KV100 . . . 36
6.4 Propeller selection . . . 37
6.5 Power supply . . . 38
7.1 Calibration of T-motor U8II KV100 . . . 43
7.2 The Blade Element Momentum Theory . . . 45
7.3 Thrust range efficiency . . . 45
7.4 28U 28L . . . 46
7.5 28U 30L . . . 47
7.6 28U 32L . . . 47
7.7 30U 30L . . . 48
7.8 30U 32L . . . 48
7.9 32U 32L . . . 49
7.10 Maximum thrust . . . 51
7.11 Minimum thrust . . . 51
7.12 Average thrust . . . 52
7.13 Hovering thrust . . . 52
7.14 Optimizing for angle of attack . . . 53
7.15 Optimizing for angle of attack for pitch inside the exhaust area . . . 54
8.1 Coaxial performance with 2500 rpm . . . 56
8.2 Hovering Thrust . . . 56

List of Tables

6.1 Design specifications RC Benchmark series 1780 35
6.2 Test plan, Z_i for i = 0, 1, 2, 3, 4 40
6.3 Propeller spacing 41
7.1 Efficiency difference, changing distance 50
7.2 Percent efficiency change for different propeller configurations 50
8.1 Thrust range from 20% to 80% scenario 59
8.2 Hovering scenario 59

Nomenclature

Acronyms	Description	Units
UAV	Unmanned aerial vehicle	
UiS	University of Stavanger	
rpm	Revolutions per minute	min^{-1}
T	Thrust	N
BEMT	Blade element momentum theory	
BET	Blade element theory	
SMT	Simple Momentum theory	
r	Radius	m
Z	Distance between propellers	mm
Pitch	Angle between blade and horizontal line	radians
ϕ	Angle between horizontal line and total velocity direction	radians
α	Angle between blade and total velocity direction	radians
V_∞	Forwards Velocity	m/s
V_Ω	Rotational velocity	m/s
C_T	Thrust coefficient	
C_Q	Torque coefficient	
C_d	Drag coefficient	
C_l	Lift coefficient	
dF_T	Difference in tangential force	
dF_d	Difference in drag force	
dF_N	Difference in normal force	
dF_l	Difference in lift force	
σ	Rotor solidity	
V	Forwards Velocity including the induction factor	m/s
V´	Rotational velocity including the induction factor	m/s
a	axial induction factor	
a'	angular induction factor	
U	Combined velocities	m/s
Δ T	Difference in thrust	N
Δ Q	Difference in torque	N/m
p	Pressure	Pascal
P	Power	Watt
dr	difference in radius	mm
ρ	Air density	kg/m^3
A	Blade surface area	mm^2
A_s	Exhaust blade surface area	mm^2
V_i	Initial wind velocity	m/s
V_s	Exhaust wind velocity	m/s
C_s	Wake correction factor	
B	Number of blades	
μ	Dynamic viscosity	Kg/ms

1 Introduction

Ever since the Wright brothers first produced the first plane that had enough lift to take off with humans on board, humans have been restricted to either using a plane or a helicopter for aerial flight. More specifically, humans could choose between machines utilizing vertical take-off or horizontal take-off. In later years more and more refined versions of the helicopter have been developed and today we have what is called unmanned aerial vehicles, UAVs as they are often called, or more commonly known as drones. UAVs are, as the name suggests, unmanned vehicles for flight, controlled by either remote pilots, GPS or via specialized software [1].

Historically drones have seen their main use in the military sector, but in later years they have been refined for different purposes in the industry and the civilian market. Today, many may first think of them as being primarily used by hobbyists and photographers, but that is not the case. Large corporations like Amazon [2] have specialized drones used for fast delivery of goods, IKM [3] uses them for inspection of testing equipment and companies like Nordic Unmanned [4] have found their nichè designing and customizing drones for several different uses in many different industries.

Nordic Unmanned supplies different drones developed for different tasks; this thesis will focus on their Staaker BG200 [5]. The Staaker BG200 is a mid-size UAV primarily used for photogrammetry, LiDAR scanning and mapping. It has a maximum take-off weight of 25 kg whereof 9 kg is its maximum payload capacity. The BG200 is a coaxial quadcopter, also known as an octocopter. Meaning it has a total of eight propellers distributed over 4 arms. The advantage of such a solution is that the counterrotating rotors cancels the net torque on the fuselage and thus the drone does not require a vertical tail rotor which is typical in traditional helicopter design.

As stated, the propellers in a coaxial drones are stacked on top of each other in pairs. This results in higher thrust than just having one propeller, having a coaxial system saves space compared to having two propellers in line. The downside of using such a solution is that the lower propellers suffer a loss in efficiency due to the fact that they operate in the fast moving

air from the upper propeller. This thesis will try to find the optimal configuration of such a system. Experiments will be conducted with different propeller sizes and distances between the propellers to try to improve the efficiency of the system and thus gain more flight time.

1.1 Scope

Modern drones have a restricted flight time, which is primarily limited by the weight of the vehicle, the capacity of the batteries and the efficiency of the propellers.

The question this work is trying to answer is: What is the optimal combination of propeller sizes and spacing between them to gain additional flight time.

1.1.1 Learning objectives

The learning objective of this bachelor thesis is to develop the ability to understand and systematically present the improvements that can be done to a coaxial quadcopter. This is done through studying the literature on the topic, performing experiments, analyzing the test data and presenting it in a bachelor thesis.

1.1.2 Performance targets

The goal of this thesis is to find the most efficient combination of propeller diameters and spacing for Nordic Unmanneds Staaker BG200 drone. From this report the participants hope to gain insight in what parameters are important to the efficiency of a modern coaxial drone.

1.1.3 Limitations

Throughout the experiments only three different propeller sizes were available to be used in the testing. Only one kind of propeller and one kind of motor which limited the scope of the testing. The sizes of the propellers being 28", 30" and 32". Originally a 29" propeller was also to be included in the testing but it was not usable due to damage. Nordic Unmanned currently uses 28" propellers on their Staaker BG200. Ideally the testing would include smaller diameter propellers in addition to the larger ones, different sized motors and propellers

with different pitch in order to uncover possible issues and to gain a better insight in how propeller size impacts performance.

The testing was performed on a RCbenchmark series 1780 [6], which allows for a single coaxial setup. This test setup does not take into account possible flow interactions between the four propeller pairs.

The testing was also only performed to simulate hover, and not forward motion. Optimally a wind tunnel would be utilized, but seeing as UiS does not currently have a wind tunnel this was unfortunately not possible.

The focus in this thesis is on the total efficiency of the propeller system and not the individual propellers. This means that as the total efficiency of the system changes measures to investigate whether that is due to specific influences in either the upper or lower propellers will not be made.

2 Literature study

Through studying the literature on coaxial configuration for drones, a gap in knowledge presented itself in regards to propeller sizing. The articles presents studies for unmanned aerial vehicle or helicopters and aircraft. The UAVs used for hobby purposes are normally using propeller ranging from 3" to 16", and helicopters used in transportation with propellers in the range of 118". Since there is a growing market for larger UAVs, there is also a growing demand for new studies. This gives an opportunity to use theory from other propeller sizes and inspect if this matches the experimental data from medium propeller sizes, ranging from 28" to 32".

Although almost every article and paper uses the unitless measurement figure of merit (FOM), this thesis is going to focus directly on efficiency. The reason for this is that it enables people who have not read up on the literature to understand the concept. Rather using efficiency as a good comparison tool, since the thesis is designed for use by Nordic Unmanned.

Through the literature study different approaches explaining the theoretical thrust from coaxial setup appeared. Last years bachelor thesis [7] used simple momentum theory(SMT). Simple momentum theory uses an integration of fluid mass, energy and momentum conservation to explain the efficiency of thrust generated, this is explained in the article Wind energy explained: theory, design and application by J. F. Manwell, J. G. McGowan, and A. L. Rogers [8]. Another approach is utilizing Blade element momentum theory, which is a combination of momentum theory and Blade element theory (BET). A quick and good explanation of BET can be found in the book Optimizing small multi-rotor unmanned aircraft: A practical design guide [9] written by S. Prior, it explains how the actual blade generates thrust. BEMT is a combination of BET and SMT, and is considered superior due to its possibility to take into account the specification of the propeller in the calculations.

It is essential to separate high and low Reynolds number configurations. The Reynolds number is a dimensionless number that expresses the ratio of inertial forces to viscous forces [10] , with high values $> 10^6$ indicating that viscous forces are small and the flow can be seen as inviscid, meaning that the viscosity of the fluid can be considered to be zero [11]. Low

Reynolds number is often cited as being $< 10^5$, where in a low Reynolds number system the viscous forces have a larger impact on the performance. The general trend is that as the Reynolds number increases the thrust increases and the power decreases, essentially meaning that the higher the Reynolds number of the system the higher the efficiency of the system. An example of a high Reynolds propeller set up would be a helicopter, and a drone is usually a low Reynolds number layout.

Calculating the Reynolds number as a range spanning from the 28" propeller at 2000rpm to 32" propeller at 3000rpm, using values for the chord and speed calculated at the 70 % span section. This differs a bit from the method used by R. W. Deters, G. K. Ananda and M. S. Selig [11] as they used the chord and speed at the 75 % span section.

$$R_e = \frac{\rho V c}{\mu} \tag{2.1}$$

Where c is the chord of the airfoil, V is the airspeed, ρ is the density of the fluid and μ is the dynamic viscosity coefficient.

Using the values T equals 300K and p equals 1 atm to find the value for the dynamic viscosity and density, and using the range of 2000-3000 rpm gives Reynolds values for the 28" and 32" propellers in the range of:

$$R_e(28"2000rpm) = 275393 \tag{2.2}$$

$$R_e(32"3000rpm) = 545391 \tag{2.3}$$

Testing on small-scale airfoils has revealed that when operating with a Reynolds number from 40 000 to 500 000 the lift decreases and the drag increases, with a critical point of $<$100 000 [11] where the effects are particularly pronounced. Considering that the thrust is dependent on the lift, and the power is influenced by the drag, this means that the efficiency is highly influenced by the Reynolds number, and particularly has to be considered when

operating below 100 000. Seeing as the Reynolds number for this system is in the range of 275393-545391 thus is above the critical point and the effects of the Reynolds number on the system is out of the scope of this thesis these effects will not be considered further.

The propeller spacing is an essential feature to optimize in a coaxial setup. Multiple studies have been done on this parameter on both high and low Reynolds setups. The goal of optimizing the spacing between the rotors is to minimize the aerodynamic interference between the rotors. F. Bohorquez states in his dissertation on a low Reynolds drone that a 5 % gain in thrust can be gained in coaxial drones by optimizing the spacing [12].

2.1 Propeller configurations

Blade configurations appeared through literature studies to be interesting. Cédric Martins Simões states in his study[13], "Regarding propeller sizes ranging from 12" to 14", that the two scenarios that affect the efficiency in a positive way are larger propellers and a large propeller on bottom and smaller on top". If this statement is true for larger propeller sizes, remains to be investigated.

Leishman states that "The momentum theory suggests that the minimum induced losses for coaxial rotors is attained when the lower rotor operates in the fully developed slipstream of the upper rotor and at equal and opposite torque to the upper rotor" [14]. With this statement Leishman proposes that the optimal spacing between rotors in a coaxial setup is the point where the cone shaped exhaust from the upper propeller has reached the slimmest point.

For one propeller the flow creates one half of a cone shape illustrated in figure 2.1, two propellers creates two cone shapes stacked on top of each other. In the BEMT theory the second propeller operates in the fully developed slipstream of the upper propeller, this is called Vena Contracta [14]. The air from the slipstream creates a contaminated area that the second propeller has to operate in, this makes the second propeller less efficient. The slipstream area, if the slipstream is fully developed, is calculated to be $A_s = \sqrt{2}A$[14]. This area parameter is going to change when changing propeller configuration and distance between the propellers.

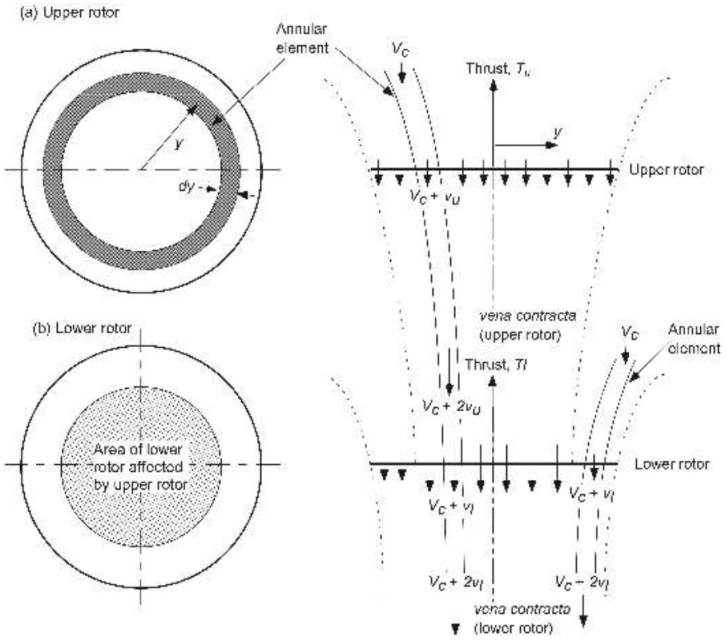

Figure 2.1: Affected area [14]

As stated previously the lower propeller operates in the exhaust from the upper propeller. This exhaust, or slipstream, is a cone-shaped volume of fast moving air particles illustrated in figure 2.1. Because it is cone shaped the crossectional area in which it hits the lower propeller varies with the size of the upper propeller and the distance between the propellers. The area with fast moving particles is often called the annular area, and the annular area decreases in size when the upper propeller decreases in size and the distance is increasing.

The degree to which the propeller is affected, depends on the size of the annular area and the speed of the particles moving through this area. C. Simões states in his study [13], that the larger the propeller sizes the better the efficiency. This effect can be a result of the propeller size and the size of the area that has not been affected by the slipstream.

2.2 Propeller spacing

By itself, optimal rotor spacing is often noted in the literature to provide for a relatively small gain in total thrust in a coaxial setup. F. Bohorquez [12] found a 5 % gain when all other

parameters being unchanged. $h/r_p \geq 0.357$ [15] is a number often used, both F. Bohorquez and Q. Quan are using this as a defining parameter when assessing the propeller spacing, r_p and h are illustrated in figure 2.2.

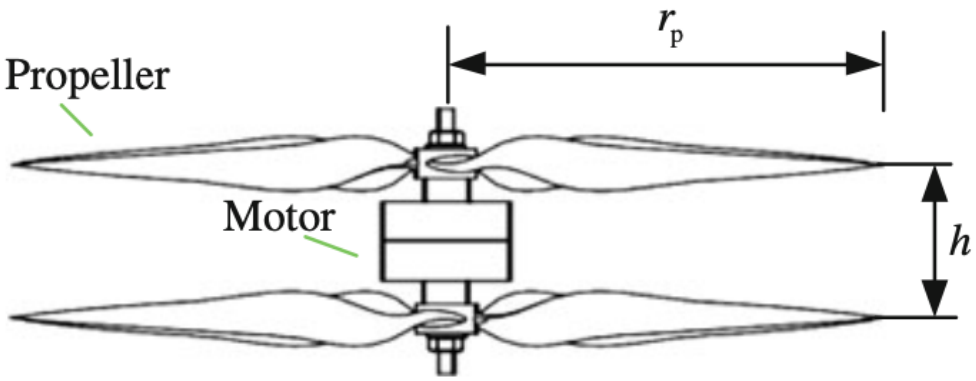

Figure 2.2: Propeller spacing [15]

Our hypothesis is that the small upper propeller and a larger size lower propeller will give a lower particle speed and a smaller contaminated annular area. Consequently leading to a greater propeller efficiency for the lower propeller and a greater overall efficiency.

3 STAAKER BG-200

The Staaker BG200 is a coaxial quadcopter, the drone is shown in figure 3.1. In today's setup the BG200 utilizes eight 28"x9.2" propellers, meaning the propellers are 28" in diameter and has a pitch of 9.2". The pitch describes the vertical displacement per horizontal rotation. The blades have a separation of 109.2 mm.

The BG200 has a "dry-weight" of 8.5 kg and two different battery options, 44 Ah and 32 Ah weighing 10.1 kg and 7.5 kg respectively. The maximum take-off weight is 25kg allowing for a 6.4 kg payload in the 44 Ah configuration and 9kg in the 32Ah configuration.

The drone has a theoretical maximum flight time of 66 minutes with the 44 Ah battery and no payload. The flight time is calculated using a theoretical model not taking variables like wind, air temperature and moisture into account, so real flight time might differ.

Many variables influence the flight time of the drone. The flight time is directly proportional to the efficiency of the system, and the efficiency is influenced by the efficiency of the motors, the weight, the rotor configuration, the propeller characteristics and the horizontal separation between the propellers.

As stated the BG200 utilizes eight 28"x9.2" rotors, but the drone can also be modified for three other rotor options to choose from, 29"x9.5" 30"x10.5" and 32"x11".

Figure 3.1: Staaker BG200 [5]

4 Theory

In order for any object to leave the ground, the upward forces needs to exceed the downward force of gravity. Drones uses lift to exceed gravity creating thrust and propel itself in any direction. In short terms the objective for this thesis is to improve thrust and find the optimal setup for thrust per power used, with units Newton per watt. For further reference thrust per power unit is called propeller efficiency.

This theory chapter will present relevant theory that will be used in the paper to answer the hypothesis. The theory chapter is sectioned into four parts. The first part is explaining simple momentum theory, a theory that uses fluid mass, energy and momentum conservation in 2D to describe the thrust. The second part using blade element theory to describe how drone propellers work, by a motor applying torque and the blade generating thrust. The third part, is looking at the two theories together to explain the blade element momentum theory(BEMT), describing the effect rotational speed has on Δ thrust and Δ torque. Afterwards, explaining how the upper blade affect the lower. The last section is the optimization section, where efficiency is explained.

4.1 Simple momentum theory

Simple momentum theory does not take into account the flow around the surfaces, in other words, the model is 2D and does not take into consideration the blades geometry just the size. This model based on a linear momentum theory, and a controlled volume. The assumption that the air flow has no rotation is valid in the first section, this assumption is removed at a later point. The equations and principles in this sub chapter are from the J.F Manwell and J. G. McGowan book Wind Energy Explained[8], although this book is designed for wind turbines the same principle applies to UAVs. The first step is to calculate the thrust from the change of the air particle speed. The air stream for one propeller is illustrated in figure 4.1. From the conservation of linear momentum for one dimension the thrust is equal to the rate of change of the momentum air stream, expressed in equation (4.1).

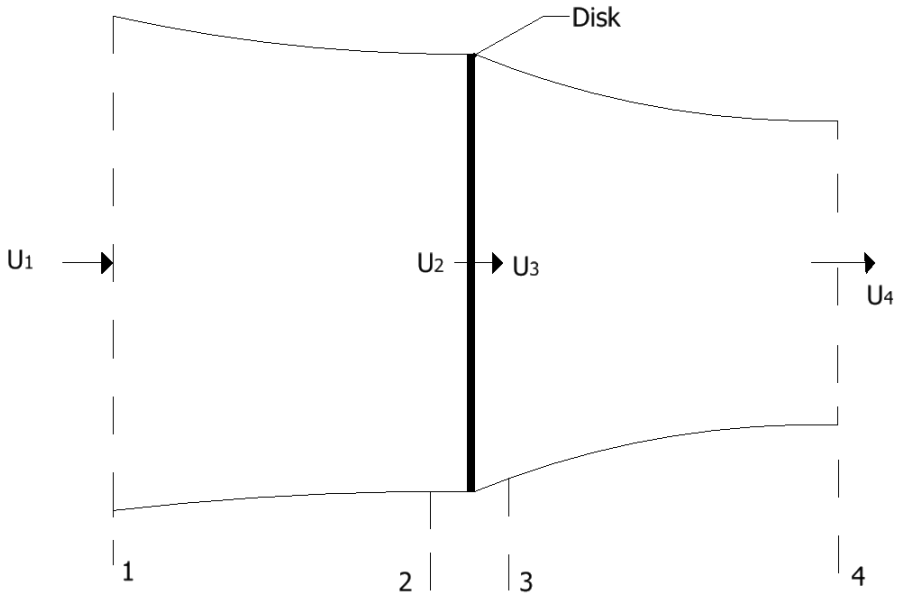

Figure 4.1: Actuator disc model [8]

$$T = U_4(\rho A U_4) - U_1(\rho A U_1) \tag{4.1}$$

For steady state flow the $(\rho A U_1) = (\rho A U_4) = \dot{m}$, (4.2) is a simplification of equation (4.1).

$$T = \dot{m}(U_4 - U_1) \tag{4.2}$$

The next step is to us the Bernoulli equations to express the thrust. The Bernoulli equations can be used on the two sides of the disc, with the assumption that the pressure $P_1 = P_4$ and the velocity over the disc remains constant $U_2 = U_3$. The result from the Bernoulli is the equations (4.3) and (4.4).

$$p_1 + \frac{1}{2}\rho U_1^2 = p_2 + \frac{1}{2}\rho U_2^2 \tag{4.3}$$

$$p_3 + \frac{1}{2}\rho U_3^2 = p_4 + \frac{1}{2}\rho U_4^2 \tag{4.4}$$

The thrust is expressed by the difference in pressure on each side of the disc and the area of the disc.

$$T = A(p_3 - p_2) \tag{4.5}$$

Solving equation (4.3) and (4.4) for $p_3 - p_2$, this results in an equation (4.6) for thrust.

$$T = \frac{1}{2}\rho A(U_4^2 - U_1^2) \tag{4.6}$$

Mass flow rate $\dot{m}$ can be expressed with $\rho A_2 U_2$ to find an expression for velocity on top of the disc U_2. The equation 4.7 expresses that the velocity on top of the disc is an average of the velocities going in and out from the disc.

$$U_2 = (U_1 + U_4)/2 \tag{4.7}$$

Using this equation one can express the axial induction factor(a). The axial induction factor(a) is a correction for the fractional increase in the wind velocity caused by the blades, and can be expressed using the velocities U_1 and U_2. As well as U_2 and U_4. Illustrated in equation (4.8)

$$a = \frac{U_2 - U_1}{U_2} \tag{4.8}$$

Combining equation (4.8) and (4.7) can an expression for U_2(4.9) and U_4(4.10) be found.

$$U_2 = U_1(1 + a) \tag{4.9}$$

$$U_4 = U_1(1 + 2a) \tag{4.10}$$

The next step is to find the power input into the motor of the drone. The power input

required to acquire a specific velocity is expressed as power equals the thrust time the velocity $P = TU$. Using equation (4.6) for the thrust equation (4.11) is obtained.

$$P = \frac{1}{2} A_2 (U_4^2 - U_1^2) U_2 \tag{4.11}$$

Extending the equation using the conjugate theorem, and substituting U_1 and U_4 using equation (4.9) and (4.10) results in the power equation (4.13).

$$P = \frac{1}{2} A_2 (U_4 + U_1)(U_4 - U_1) U_2 \tag{4.12}$$

$$P = \frac{1}{2} \rho A U_1^3 4a(1+a)^2 \tag{4.13}$$

In the same way the power was expressed the thrust can be expressed combining equation (4.6),(4.9) and (4.10) resulting in the thrust equation (4.14).

$$T = \frac{1}{2} \rho A U_1^2 4a(1+a) \tag{4.14}$$

Now the assumption that the blade does not apply rotation to the air flow, and creates angular momentum is removed. This extends the analysis to include torque ΔQ. The energy equation can be used to express the difference in torque. The relative wind between the blade and the wind difference in angular velocity can be expressed by small omega $\Omega = \Omega + \omega$. The energy equation combined with the relative wind is:

$$p_3 - p_2 = \rho(\Omega + \frac{1}{2}\omega)\omega r^2 \tag{4.15}$$

The next step is to slice the disc into sections, the reason why the rotors has to be sliced into smaller sections is that the moment of inertia changes when moving away from center. The difference in thrust on blade section can be expressed by the pressure difference and the area of the blade section. The blade section difference in area can also be expressed as the

difference in radius $dA = 2\pi r dr$. Including the difference in area results in the difference in thrust, resulting in equation (4.16).

$$\Delta T = (p_3 - p_2)dA = [\rho(\Omega + \frac{1}{2}\omega)\omega r^2]2\pi r dr \tag{4.16}$$

As for the axial induction factor one also need an angular induction factor(a'). The angular induction factor(a') is a correction for the fractional increase in the angular velocity caused by the blades, and is expressed in equation (4.17).

$$a' = \frac{\omega}{2\Omega} \tag{4.17}$$

The next step is to calculate the difference in torque. This is done by using the conservation of angular momentum. For the scenario where a motor applies torque onto the blade, the change in torque equals the change of angular momentum and results in equation (4.18).

$$\Delta Q = \Delta \dot{m} \omega r^2 = (\rho U_2 2\pi r dr)\omega r^2 \tag{4.18}$$

Combining equations (4.17),(4.18) and (4.9) result in the difference in torque illustrated in equation (4.19).

$$\Delta Q = 4a'(1 + a)\rho U \Omega r^3 \pi dr \tag{4.19}$$

Change in thrust can be expressed using axial induction factor, the result is.

$$\Delta T = 4\rho U^2 \pi (1 + a) a r \Delta r \tag{4.20}$$

The next step is to take a deeper dive into the wind affect on the disk. The winds into the blade is illustrated in figure 4.2, v_∞ is the incoming wind into the system, which represents U_1 in the earlier explanation of induction factor. V_Ω represent the wind occurring from the

rotation of the blade, represented by $r\Omega$ in the explanation of axial induction factor. As one can see in the figure there is an extra small vector, this represent the induction factors that was explained earlier.

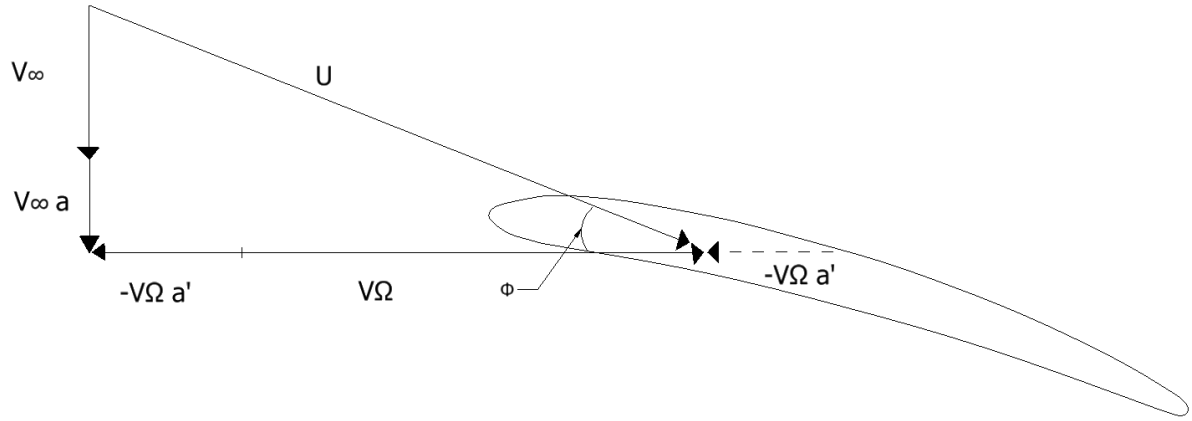

Figure 4.2: Wind velocity vectors

The result of vector summation gives V and represents the wind into the system including the induction factor(a). V' representing the wind occurring from the rotation including the angular induction factor(a') of the blade and is calculated from vector subtraction.

$$V = V_\infty + V_\infty a = V_\infty(1 + a) \tag{4.21}$$

$$V' = V_\Omega - V_\Omega a' = V\Omega(1 - a') \tag{4.22}$$

Finding the relative wind for the airfoil(U) is found by Pythagoras illustrated in equation (4.23). Dr. Knut Erik. T. Giljarhus have used V_Ω, V_∞, U, v_s, v_i in his script and theory description [16, 17] and these are the terms that is going to be used in the rest of the theory chapter and thesis.

$$U = \sqrt{V'^2 + V^2} \tag{4.23}$$

Equation (4.24) and (4.25) are equation (4.20) and (4.19) using the terms used in the pyBEMT, where $U_1 = v_\infty$.

$$\Delta T = 4\pi\rho V_\infty^2(1+a)ar\Delta r \tag{4.24}$$

$$\Delta Q = 4\pi\rho r^3 V_\infty \Omega(1+a)a'r\Delta r \tag{4.25}$$

These two equations for ΔQ and ΔT are going to be used later in the blade element momentum theory section.

4.2 The blade element theory

The blade element theory is used to analyze the aerodynamical performance of the airfoil, by using the foundations that was explained in the simple momentum theory. The end goal is to end up with an equation for ΔQ and ΔF_N.

Airfoil is the cross sectional shape of the propeller, the pressure difference around the airfoil generates lift. The equations and principles in this sub chapter are a combination of the J.F Manwell and J. G. McGowan book Wind Energy Explained [8] and dr. Knut Erik. T. Giljarhus´ pyBEMT model [17, 16]. The first step is to cut the blade into sections illustrated in figure 4.3, each airfoil has specific geometrical properties. The properties that affect the thrust and torque are chord(c), radius(dr), angle of attack(α), pitch(p) and angle of relative wind(ϕ).

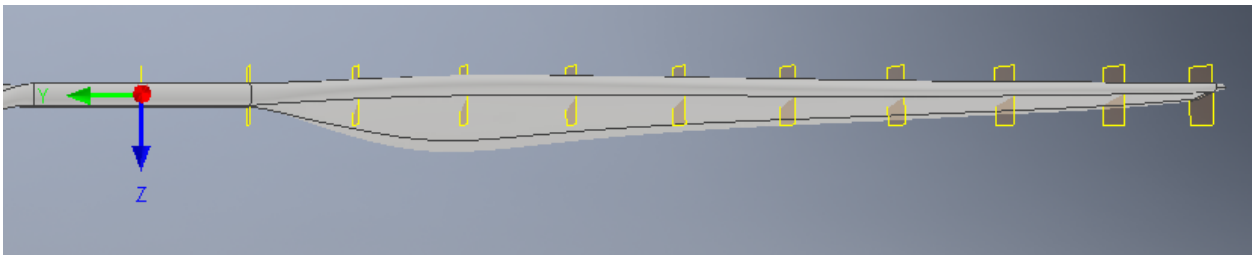

Figure 4.3: Blade section

As mentioned in the chapter about limitations, UiS does not have a wind tunnel. As a consequence this thesis will not take V_∞, in as a parameter when comparing the theory with experimental data. The second blade have wind from the upper so the concept of V_∞ still needs to be explained. Figure 4.4 shows the relative wind(U) is the vector summation of the wind speed($V_\infty(1+a)$) and the rotational wind speed($V_\Omega(1-a')$). The angle ϕ is the angle between the relative wind and the rotational plane. The induced factors are the same as in the subsection simple momentum theory. The relative wind between the wake and the blade at the rotor plane can be expressed, using the induction factor, with $\Omega r + \omega r/2 = \Omega r(1+a')$. From these two vectors $V_\infty(1+a)$ and $V_\Omega(1-a')$ one can find the trigonometrical solution for $\tan\phi$, resulting in equation (4.26) This equation is going to be used in BEMT sub chapter. To easier explain the BET model a step through guide has been implemented.

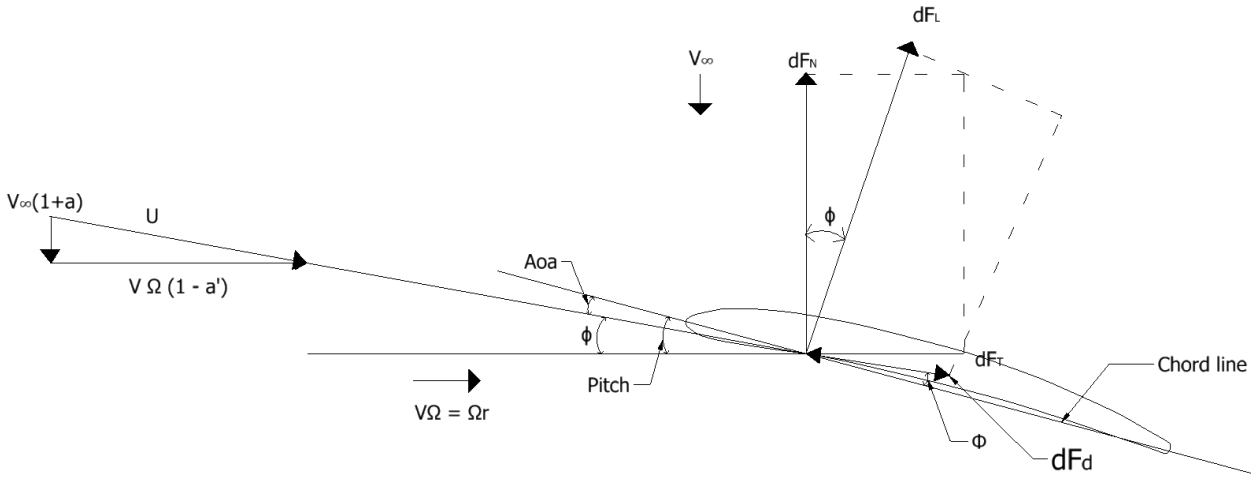

Figure 4.4: Loads acting on airfoil [8]

$$tan(\phi) = \frac{(1+a)V_\Omega}{(1+a)V_\infty} \tag{4.26}$$

Step one in finding the equation for change in thrust and torque is to find an equation for the change in tangential force and normal force. The tangential force is the force generated by the motor applying torque to the blade. The normal force is the force that the blade applies to the air particles to generate velocity. The lift and drag coefficients can be expressed using the definition of drag and lift coefficients equation (4.27) and (4.28).

$$C_l = \frac{L}{\frac{1}{2}\rho U^2 c} \tag{4.27}$$

$$C_d = \frac{D}{\frac{1}{2}\rho U^2 c} \tag{4.28}$$

Where L is the lift force and D is drag force, ρ is the air density, U is the relative wind velocity and c is the chord length of the airfoil. Expanding D to dF_D/dr and L to dF_L/dr and solving equation(4.27) and (4.28) for dF_D and dF_L gives equations:

$$dF_L = \frac{1}{2} C_l \rho U^2 c dr \tag{4.29}$$

$$dF_D = \frac{1}{2} C_d \rho U^2 c dr \tag{4.30}$$

The second step is to express the change in normal and tangential force by the lift and the drag. The difference in the normal forces is a vector summation of the difference in the lift force projected onto the vertical plane, subtracted by the difference in the drag force projected onto the vertical plane resulting in equation (4.31). The same principles works for the tangential force. The forces is projected onto the horizontal plane and the vector summation and the result is equations (4.32).

$$dF_N = dF_L \cos\phi - dF_D \sin\phi \tag{4.31}$$

$$dF_T = dF_L \sin\phi + dF_D \cos\phi \tag{4.32}$$

The third step is to put equation (4.29) and (4.30) into the equation (4.31) and (4.32), to get an expression for the normal and tangential force using coefficients, relative velocity, density, chord and change in radius. Resulting in equations (4.33) and (4.34),

$$dF_N = B\frac{1}{2}\rho c U^2(C_l \cos\phi - C_d \sin\phi)\delta r \tag{4.33}$$

$$dF_T = \rho c U^2(C_l \sin\phi + C_d \cos\phi)\delta r \tag{4.34}$$

The final step is to take into account that the tangential force works at an distance(r), and is given by equation (4.35), and including equation (4.34) resulting in equation (4.36).

$$\Delta Q = B r dF_T \tag{4.35}$$

$$\Delta Q = B\frac{1}{2}\rho c U^2(C_l \sin\phi - C_d \cos\phi)dr \tag{4.36}$$

4.3 The blade element momentum theory

Blade Element Momentum Theory combines the momentum theory and blade element theory. Blade Element Theory is used to calculate the loads on the blades at various speeds, and from the loads calculate the thrust and power consumed by the motor. Step one in the process of explaining the BEMT model is to combine the equations from simple momentum theory and blade element theory, where $\Delta Q = \Delta Q$ and $\Delta T = dF_N$.

The expressions from the simple momentum theory are.

$$\Delta T = 4\pi\rho V_\infty^2(1+a)a r dr \tag{4.37}$$

$$\Delta Q = 4\pi\rho r^3 V_\infty \Omega(1+a)a' r dr \tag{4.38}$$

The expressions for the blade element theory are.

$$dF_N = \rho c U^2 (C_l \cos\phi + C_d \sin\phi) dr \tag{4.39}$$

$$\Delta Q = \rho c U^2 (C_l \sin\phi - C_d \cos\phi) dr \tag{4.40}$$

To make the equations more comprehensible two coefficients are created illustrated in equation (4.41) and (4.42), these two coefficients were added to equation (4.39) and (4.40).

$$C_T = C_l \cos\phi - C_d \sin\phi \tag{4.41}$$

$$C_Q = C_l \sin\phi + C_d \cos\phi \tag{4.42}$$

The second step is to to solve the thrust equations (4.37) and (4.39) for the induction factor (a).

$$a = \frac{1}{\frac{4\sin^2\phi}{\sigma C_T} - 1} \tag{4.43}$$

Rotor solidity (σ) takes geometric properties as parameters, chord(Bc) in equation (4.44) is the length of the airfoil times the number of blades and r is the radius. σ is the rotor solidity and is the fractional area occupied by the blade.

$$\sigma = \frac{Bc}{2\pi r} \tag{4.44}$$

The third step is to solve the torque equations (4.38) and (4.40) for the angular induction factor (a').

$$a' = \frac{1}{\frac{4\sin\phi\cos\phi}{\sigma C_Q} + 1} \tag{4.45}$$

Step four is to solve equation (4.26) for the angle ϕ, this equation has two unknown. The solution is an iterating process, in pyBEMT [16, 17] this process is solved by using root-finding functions from the SciPy. The first step is to set a and a' = 0, compute the angle of the relevant wind ϕ, then compute the angle of attack α using equation (4.46). Angle of attack (α) is the angle between the relative wind and the chord line illustrated in figure 4.4. The optimal propeller design would be to have angle of attack equal to 0, this is going to be investigated in the optimizing propeller chapter.

$$\alpha = \phi - pitch \tag{4.46}$$

Step five is to find the lift ($C_l(\alpha)$) and drag coefficients($C_d(\alpha)$). The lift and drag coefficients are found through tables specific to the airfoil and angle of attack, pyBEMT have airfoil tables stored in folders. Pitch is a geometric property that varies from blade section to blade section.

$$C_T = C_l\cos\phi - C_d\sin\phi \tag{4.47}$$

$$C_Q = C_l\sin\phi + C_d\cos\phi \tag{4.48}$$

$$\sigma = \frac{Bc}{2\pi r} \tag{4.49}$$

Step six is to calculate the induced factors in equation (4.51) and (4.52). To accomplish this one has to calculate the thrust and torque coefficient using equations (4.47) and (4.48) and the rotor solidity(σ) using equation (4.49). The B in solidity equation is the number of blade, all the propellers for drone Staaker BG200 has two blades.

$$a = \frac{1}{\frac{4\sin^2\phi}{\sigma C_T} - 1} \tag{4.50}$$

$$a' = \frac{1}{\frac{4\sin\phi\cos\phi}{\sigma C_Q} + 1} \tag{4.51}$$

Step seven is to check if the assumed induced factors were correct. If the induction factors changes more than a specific tolerance from the induced factors in step four, the process from step four has to be redone including an increase in induction factors. The equations in this part are derived from a combination of J.F Manwell and J. G. McGowan book Wind Energy Explained[8] and Dr. Knut Erik T. Giljarhus´ pyBEMT theory [16, 17].

The final step is to calculate the change in thrust and torque by calculating the sectional value. Then finding the mechanical power that needs to be supplied with equation (4.52), and adding the sectional values together to get the total thrust generated by the torque. This process is not practically possible by hand, to solve this the python script pyBEMT from Dr. Knut Erik T. Giljarhus [16, 17] was used.

$$\Delta P = \Omega \Delta Q \tag{4.52}$$

4.4 Coaxial setup

Staaker BG200 uses a coaxial setup, this results in the wake from the upper propeller reduces the efficiency for the lower propeller. Figure 2.2 shows that the slipstream from the first propeller goes in to the second one and reduces the efficiency. One of the stated criteria for the blade element momentum theory model is that slipstream needs to be fully developed, this phenomenon is called Vena Contracta. According to J. G. Leishman and S. Ananthan article [14] Vena Contracta is where that the slipstream is fully developed and the radius of the area is $r_s = \frac{r}{\sqrt{2}}$. The speed of the particles are derived from the continuity equation (4.53).

$$V_s \pi r_s^2 = V_i \pi r^2 \tag{4.53}$$

The thrust generated from the upper propeller equals the change in momentum equation (4.54).

$$T = \rho V_i A V_s \tag{4.54}$$

The work done by the upper rotor equals to the kinetic energy in the slipstream, resulting in equation (4.55).

$$T V_i = \rho V_i A V_s^2 \tag{4.55}$$

The next step is to solve equation (4.55) for V_s, and add a wake correction factor C_s to adjust for unknowns variables which helps aligning the mathematical model with experimental results.

$$v_s = C_s \sqrt{\frac{2T}{\rho A}} \tag{4.56}$$

$$V = V_\infty + V_\infty a + v_s = V_\infty (1 + a) + v_s \tag{4.57}$$

The final step to calculate the total thrust(ΔT) generated by the motor, is to calculate the thrust and torque from the upper blade through the steps in the BEMT step model. Then calculate the particle speeds generated from the upper rotor, using the thrust from the upper propeller to calculate the exhaust air particle speed. Using the exhaust, equation (4.57), particle speed in equation (4.56) and starting the BEMT step through model again with the value from the new U from equation (4.23). Adding the exhaust section from the lower propeller to the sections that are not exposed to the exhaust. In the pyBEMT model there is 7 sections, out of 10 sections in total, that is exposed to the exhaust. Adding the upper and

lower propellers ΔT, ΔP and ΔQ to get the total thrust and power.

The process of calculating ΔT, ΔP and ΔQ is not practically possible to do manually, a computer program is needed to take all the sections and calculate the variables for every rpm. Our thesis used pyBEMT [16, 17] which was designed by Dr. Knut Erik T. Giljarhus, from the values calculated plots was made and are going to be presented in the result chapter. The equations presented in this chapter is from Dr. Knut Erik T. Giljarhus´ theory pyBEMT [16, 17] and J.G Leishman and S. Ananthan article [14]. Some modifications were made and are going to be explained in the Geometry chapter. The effect of the blade tip is not a part of the bachelor experimental scope, this is why the theory of the tip speed loss is not a part of the theory chapter.

4.5 Efficiency

Efficiency is a measurement of the thrust that is generated by the energy provided into the system. Efficiency is used to calculate the flight time of the drone, since the goal of this thesis is to improve the flight time, improving the efficiency is the end goal. In this thesis the focus in theoretical section of this thesis will be mechanical efficiency and the experimental section will focus electrical efficiency.

Motor efficiency is per definition how efficient the motor utilizing using electrical energy. The RCbenchmark computer program computes motor efficiency automatically into the CSV. The difference between the mechanical efficiency and electrical efficiency is the motor efficiency. Electrical efficiency is the consumption of electrical energy the motor has to produce thrust on different rotational speeds measured in watts, this is the efficiency that was used in the experiments.

Mechanical efficiency is the efficiency of the propeller to produce thrust, derived from thrust(T) divided by Torque(Q) times rotational velocity(Ω) illustrated in equation (4.58). Mechanical efficiency is what the theoretical model uses, since the theory cant take into account the lose of energy specific for each motor.

$$Mechanicaleffiency = \frac{T}{Q\Omega} \tag{4.58}$$

5 Geometric description of propeller

The BEMT model has blade specific requirements of input such as diameter, radius of the center hub, blade section, radius, chord and pitch. Figure 5.1 shows a screenshot of the inputs into the pyBEMT script. To improve the model and get a better result in the theoretical calculations a geometric description of the propeller is needed. Two different methods were used, 3D scanning and digitization from slices cut from a damaged propeller.

```
[rotor]
nblades = 2
diameter = 0.762
radius_hub = 0.07
section = GOE_450 GOE_450 GOE_450 GOE_450 GOE_450 GOE_450 GOE_450 GOE_408 GOE_408
radius = 0.0384 0.07688 0.1153 0.1538 0.1922 0.2307 0.2688 0.3072 0.3456
chord  = 0.032 0.062 0.0717 0.0732 0.0685 0.0617 0.0531 0.0433 0.0372
pitch =0 17.7 18.25 15.6 12.9 10.56 9.36 8.51 8.54
```

Figure 5.1: BEMT input requirements [16, 17]

5.1 3D-Scanning

In order to obtain the necessary variables needed for the pyBEMT model from the propellers, the chord and pitch. The manufacturer was contacted to try and obtain the original 3D files from them, but seeing as many manufacturers of such parts deem the geometry as trade secrets, T-motor were not willing to sharing that information. Thus it was determined to make an attempt at 3D scanning the 30" propeller, the process is illustrated in figure 5.2. Assuming T-motor have used the same model on each propeller just scaling it to fit the needed diameters. The same procedure was used in this approach, scanning a 30" propeller because this gave the worst pyBEMT results.

3D laser scanning is a process in which a laser line is projected on the part in question and cameras record how the line changes in distance and shape in three dimensions as the line passes over the part. This produces a 3D cloud of points representing the surface of the scanned part. This point cloud can then be converted into the desired format, depending on what the scanned data is to be used for. In this case a Creaform handyscan 700[18] was

used for the scanning and the point cloud was converted into a mesh file. A mesh file is a file containing vertices, polygons and faces that defines the surface of a model.

Figure 5.2: 3D-Scan

Once the raw mesh files were obtained, because of the complex geometry, it appeared that the scan had issues. The model had multiple holes, was missing the reference center hole and was lacking important geometry from the lead and trailing edge which makes estimating the chord and pitch difficult. Multiple attempts in both Fusion360 and Autodesk Inventor at repairing the geometry was attempted. The full 3D scanned mesh is illustrated in figure 5.3, and a closer zoom is illustrated in 5.4 were the holes in the surface and the leading edge can be observed.

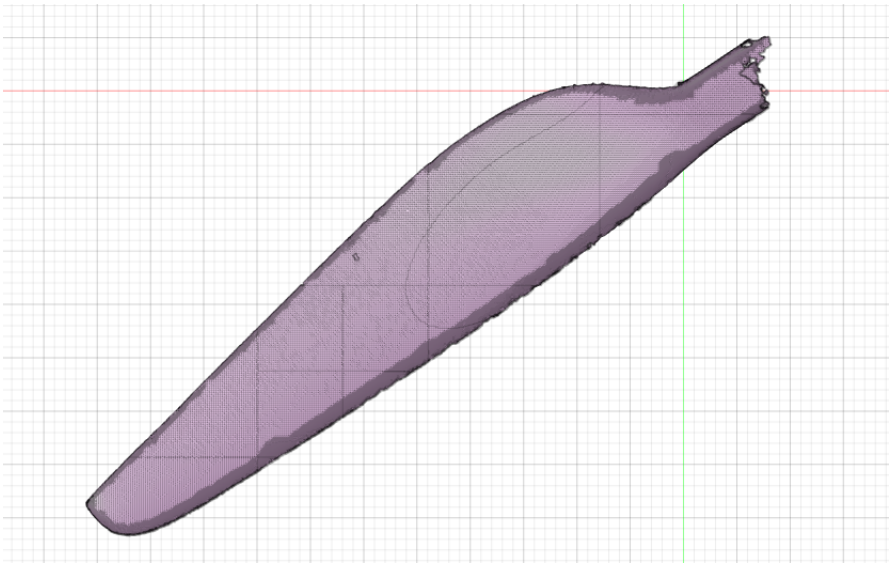

Figure 5.3: 3D scanned mesh of propeller

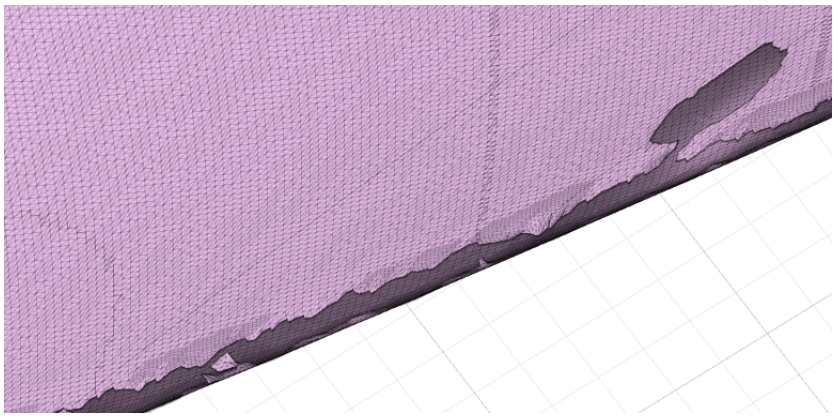

Figure 5.4: Zoomed in 3D scanned mesh

Attempts included using T-spline algorithms, filling and smoothing algorithms and simply trying to convert the mesh to solid in both Fusion360 and Autodesk Inventor to no avail. A complete solid model could without a doubt be made from the mesh by simply guesstimating the lacking geometry, but most likely too much information would have been lost. Specialized software that repairs such flaws to an engineering degree of certainty do exist, but are expensive and out of the scope of specialization for this work.

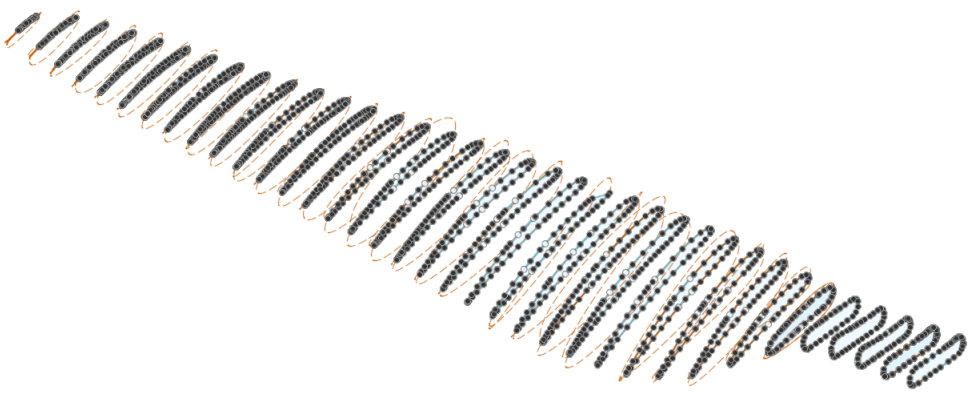

Figure 5.5: 3D sections

5.2 Cutting of propeller

After the issues with the scanned files, it was determined that a simpler approach to attaining the variables was needed in order to complete the necessary pyBEMT calculations. Seeing as one of the 28" propellers was taken out of service due to crack formation, an attempt at sawing it into sections and directly measure the chord and pitch at the necessary points, and creating digital points around the outline of the airfoils. This Outline was handed over to Dr. Knut Erik T. Giljarhus in an attempt of finding the correct lift and drag coefficients. As well as increasing the accuracy for the pyBEMT model the cutting of the propeller was also done to assist the master student, writing for Nordic Unmanned, to create a solid propeller model and get a more accurate result in his simulations. An attempt of aligning the sections is illustrated in figure 5.5. The priority of finishing the bachelor thesis came in the way of finishing the propeller model. After sending Dr. Knut Erik T. Giljarhus the outline of the airfoils he took over the process.

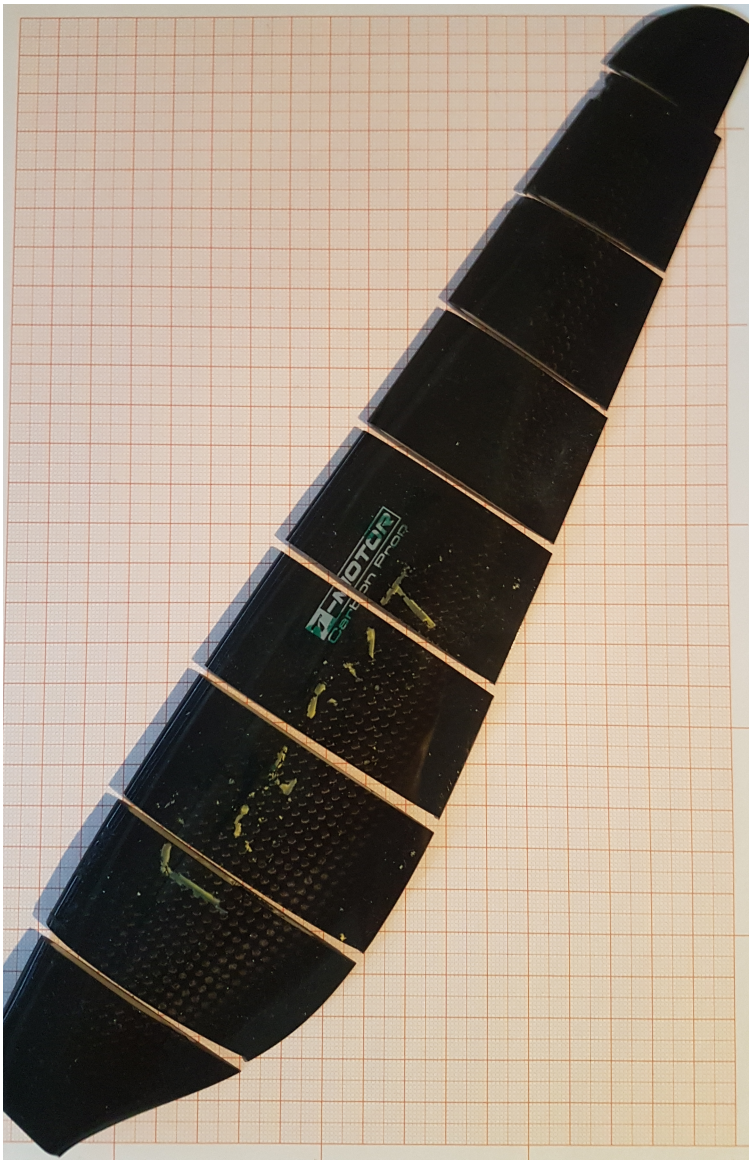

Figure 5.6: Propeller cutting

The operation of cutting the propeller had to be carried out with great care as carbon fiber is a hard and brittle material and the propeller already had cracks. Thus it was important to come up with a good procedure for the cutting before commencing to avoid scrapping the sample, the outcome from cutting the propeller is displayed in figure 5.6.

5.3 Pybemt

PyBEMT is a python script that takes inputs and calculates thrust and mechanical power using the BEMT model. In pyBEMT the blade is divided into ten different pieces. Every piece is called a section. The sections has individual geometry, therefore Dr. Knut Erik T. Giljarhus compared each section in a database to figure out what type of airfoils each section consists of. Figure 5.7 illustrates the result from comparing the airfoil with the database airfoils. The pitch is calculated from the angle of the blade piece and the horizontal line. The chord is the distance between tip to tip in the section. The rest of the parameters has been calculated.

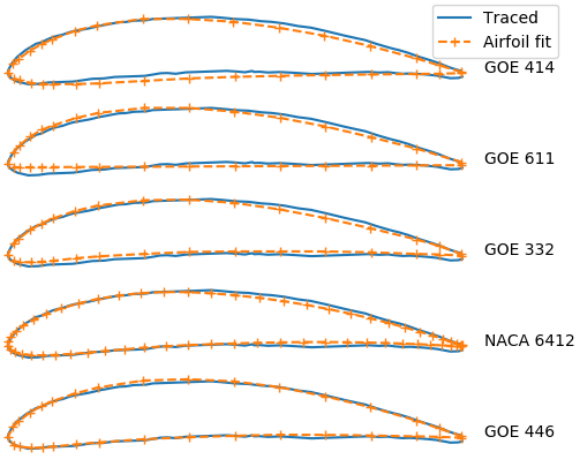

Figure 5.7: Comparison airfoil section

This pyBEMT script also has a wake correction factor called C_S, this factor is used to regulate the polluted wind speed that goes from the upper propeller to the lower propeller. The Pybemt script created by Dr. Knut Erik T. Giljarhus states that one of the conditions is that the slipstream needs to be in Vena Contracta, which means that the slip stream needs to be fully developed and the area of the slipstream needs to be $r_s = \frac{r}{\sqrt{2}}$.

The pyBEMT script, as explained in the theoretical part, takes the data through the BEMT calculation process and adds the sections thrust and mechanical power to make a graph that

is going to be presented in the result chapter.

5.4 Optimising propeller

The theory of optimizing the propeller blade is that the upper propeller blows exhaust on the lower propeller and because forward velocity the the optimal angle will change. As explained earlier, in the theory chapter the lower blade is exposed to exhaust particles(v_s) from the upper propeller since the blade has not been specifically designed for being the lower propeller in a coaxial setup the optimal pitch on the lower propeller could improvement the efficiency. The ideal procedure for finding the optimal angle would be to calculate the angle the lower propeller should be modified with. To do this one has to calculate the relative velocity with Pythagoras and calculate the induction factors, see figure 5.8 to get the illustrated picture.

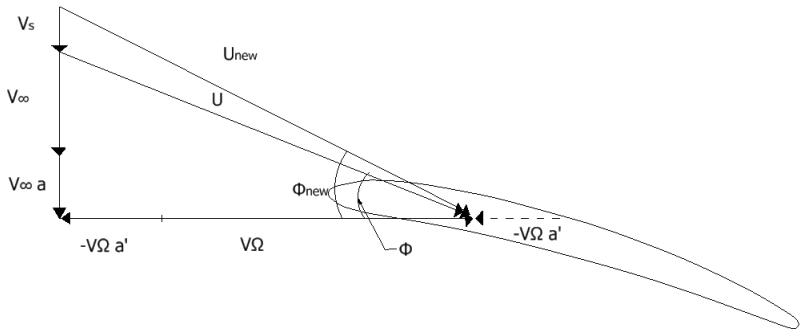

Figure 5.8: Wind velocity vectors including exhaust particles

6 Experimental setup

6.1 HMS

As stated, all the experiments were performed on a RCbenchmark test rig. The rig and associated equipment can be quite dangerous if not handled with care and precaution. Thus it requires some introduction by the lab engineers in order to be familiarized with the equipment before use.

In order to handle the test rig with proper care and to avoid harm it was deemed necessary to develop a proper procedure for the users. The group which had used the test rig the previous year had already developed a procedure [7]. However it was deemed insufficient in regards to safety and also experiment repeatability. Therefore it was determined to write a new procedure based on the old one.

The first step was to establish what kind of dangers the rig posed. The motors are capable of rotating the propellers up to more than 3000 rpm. The propellers are made from carbon fiber, which is a really hard material that can fracture and splinter. The power supplies deliver 44,4 V which is more than sufficient to pass trough the human body. Lastly the test rig also produces a lot of noise. Therefore appropriate precautions needed to be taken.

To protect the users and bystanders from these dangers it was established that the area was to be blocked off. This was done by using red tape to avoid untrained personnel from entering the zone in which the propellers could in theory shoot off if they were to come loose or fracture. Protective glasses were to be used when around the test cell as well as ear protection. When entering the test cell the power supplies for the motors and the controlboard was to be immediately turned off and the computer disconnected. This to avoid accidentally starting the propellers while someone was inside the cell.

6.2 Test setup

Per advice from Nordic Unmanned the experiments were based on a thrust range, spanning from 20 to 80 % of their current setup. This is also the range used in last years bachelor thesis [7], which is lending itself to better comparison of results between the two reports and Nordic Unmanned´s current setup. Meaning, they are per now utilizing T-motor G28x9.2 propellers, U8II KV100 motors and a spacing of 1092mm. Our benchmark testing of this setup provided us with a thrust range spanning from 24N to 99N.

As for the different propeller sizes used, 28”, 30” and 32” diameter were chosen respectively. Preliminary a 29" propeller was also to the tested but due to a fault on one of the 29” blades they were dropped from the testing.

The test setup, shown in figure 6.1 and 6.2 is supplied by RCBenchmark and is their 1780 unit consisting of two test pillars with opposing motors and sensors. This is the optimal setup for coaxial testing, lending itself to adjusting the spacing between the rotors and is fitted with all the necessary sensors for data collection.

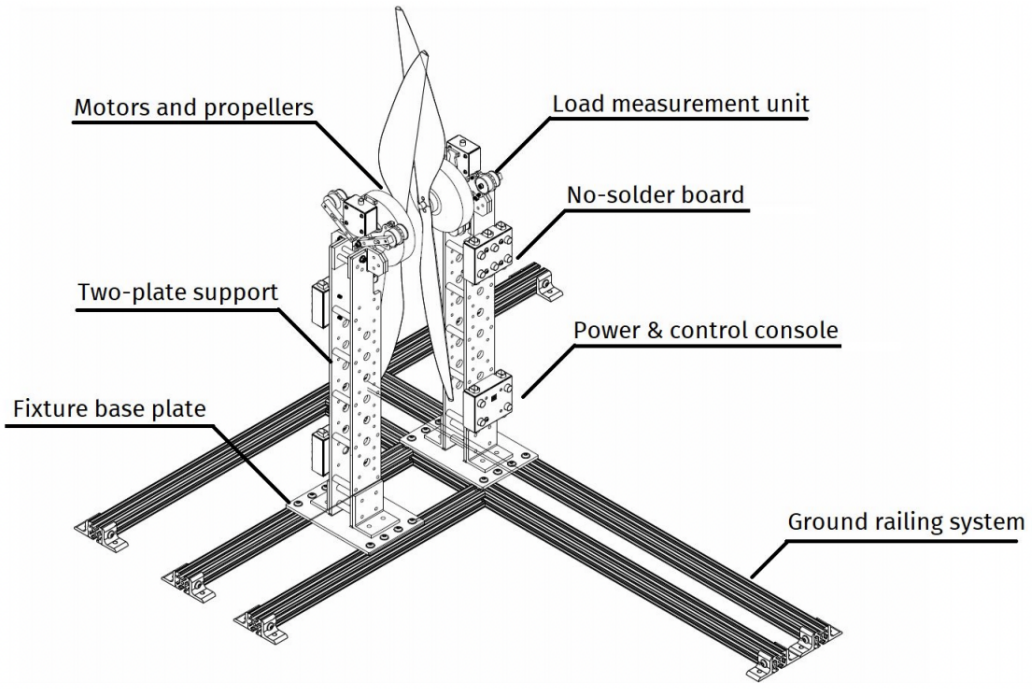

Figure 6.1: RcBenchmark series 1780 [6]

Figure 6.2: Test setup

Table 6.1: Design specifications RC Benchmark series 1780 [6]

Specification	Min.	Max.	tolerance***	unit
Thrust side A*	-25	25	±0,5 %	Kgf
Thrust side B	-25	25	±0,5 %	Kgf
Torque side A	-12	12	±0,5 %	Nm
Torque side B	-12	12	±0,5 %	Nm
Voltage side A	0	60	±0,5 %	V
Voltage side B	0	60	±0,5 %	V
Current side A	0	100	±1 %	A
Current side B	0	100	±1 %	A
Angular speed**	0	190k	-	RPM

The 1780 unit is equipped to measure rpm, torque and thrust. Table 6.1 shows the specifications and tolerances of the test rig and sensors. The RCBenchmark software allows for reading of all the sensor inputs, as well as key information such as propeller and motor efficiency.

6.2.1 Motors

The motors are supplied by T-Motor and is their U8II KV100, which is capable of a maximum power of 1406.4 W (180s) and peak current draw of 29.3 A (180s). Figure 6.3 shows how the motors are mounted to the test rig.

The motors are brushless DC-steppermotors, which is ideal in drones, as they have a long service life of 1500 flights at 40 min/flight [19] and they produce very little radio interference. The motors are rated for maximum 28 kg total weight when configured as an octocopter.

Figure 6.3: T-motor U8II KV100

The motors feature IP55 class motor protection, which is a standardized international classification of motor protection defined by IEC 60034-5. IP stands for International Protection. The 55 indicates how well it is protected against ingress of dust and water. The first 5 indicates that the motor is entirely dustproof. The second 5 indicates that the motor is protected against water jets, meaning water sprayed from all directions.

6.2.2 propellers

All the propellers used in the testing can be seen in figure 6.4. The propellers are supplied by T-motor and come from the same model range. The propellers are two bladed propellers made from carbon fiber. Carbon fiber is a material with highly suitable properties in aeronautics. Depending on the manufacturing process the strength can rival that of steel at a quarter of the density. Tree different sets of propellers was used in the testing: G28x9.2, G30x10,5 and G30x11. The G in the G28x9.2 indicates the model of propeller, in our case meaning glossy, which refers to the surface-finish of the propellers in the series. 28 is the diameter of the propeller in inches, and 9.2 indicates the pitch of the propeller, also measured in inches. The pitch describes how far forward the propeller would move in one rotation in a soft solid. The propellers are marked with L or R for left or right.

Figure 6.4: Propeller selection

6.2.3 Tachometer

The optical tachometer is provided by RCbenchmark as a feature built into the 1780 test rig. The sensors uses reflected infrared light to determine the revolutions of the motors, and the software display it as RPM. The tachometer package contains a light emitting source and a sensor. It works by constantly emitting infrared light on the motor hubs. On the hub there is mounted a small piece of reflective tape. As the motors spin, the sensor will pick up

on the reflected light once every revolution. When the frequency is logged in the software it converts from frequency to RPM for easier reading.

6.2.4 Load cell

The load cells are responsible for sensing the thrust and torque produced by the propellers. The load cells consists of three arms that attach the motors to the pillars, which are turned to face each other in order to easily adjust the distance between the propellers without obstacles. The software takes into account the orientation of the load cells and is capable of outputting a total thrust-value.

6.2.5 Power supply

Due to issues with voltage drop and a lot of time spent charging, it was determined to replace the battery packs that had originally been used to power the test rig with two adjustable DC benchtop power supplies.

The power supplies have an adjustable voltage of 0-48V and a maximum current draw of 30A which makes it optimal for providing consistent power to the test rig. Figure 6.5 shows the power supplies used.

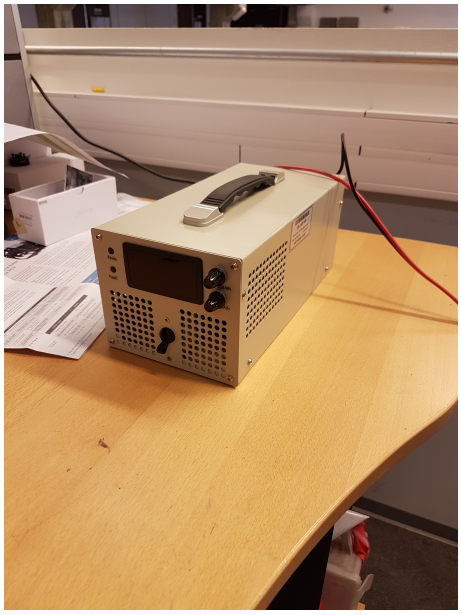

Figure 6.5: Power supply

6.3 RCbenchmark Script

The purpose of this thesis is to figure out the optimal setup for a coaxial drone Staaker BG200, by changing the variables propeller spacing and diameter. In a range between 20 and 80 % of the maximum throttle using the motor U8II KV100.

Throttle is a variable that the RCbenchmarks computer program uses and Nordic unmanned uses to operate their drones. The first problem using throttle as a driving parameter is that throttle is not linear with thrust or rpm. Secondly, throttle does not lead to a reliable result from test to test, learning from last years bachelor thesis [7] they had a thrust difference of 15 N for the same propeller configuration and distance. Therefore this thesis uses thrust as a driving parameter contrary to last year [7], when they used throttle. Thrust gives a more stable result when focusing on efficiency over different drone blades. Using thrust as the driving parameter turned out to be harder than expected. The problem was to get the total thrust from both sensors. This was solved by consulting an engineer at RCbenchmark. The response was that our script needed to call the program to find out the sensors name. Then call the sensor for the given thrust value at that moment. Consulting Jørgen Apeland, our contact from Nordic Unmanned, our goal was to create a script that tested a range from 20 to 80 % of the thrust, to give a clear picture of the efficiency between different propeller.

This lead to our script, which uses a callback function that reads the sensor and sends the value to a function called correction. Correction uses a if loop to compare the current thrust value with the target value. If the value is lower than the desired value our script ramps up the throttle by two throttle units, and the loop starts again. Throttle is the input unit the for the RCbenchmark uses to ramp up and down. When the desired value is reached, correction calls on the function called take sample which takes five data points and takes the average of this points logging it into a CSV file. Then it adjusts the desired value, while also checking if our maximum value has been reached(See appendix C).

To find the range that the script was going to operate in, a data set from the producer T-motor [19] was used to locate the 20 and 80 % mark. With this information, the test rig

was run with a single 28x9.2 propeller, which is the same propeller T-motor used in their calibration. The results were that the throttle equaled 6171 gf. This is the 80 % thrust for U8II KV100 motor. Then using two 28x9.2 propellers in a coaxial setup to find what thrust these equaled. The results were that 20 % equaled 24 N and 80 % equaled 99 N.

6.4 Test plan

To perform the testing, a test plan had to be developed. The plan needs to define the propeller spacing and the combination of propellers. As stated earlier, there was three T-motor propellers available G28”x9.2, G30”x10.5 and G32”x11, originally four, with the fourth being a G29"x9.5.

Due to some issues with crack formation on the 29" propellers, they were deemed unfit for use, and thus was eliminated from the testing. The reason being that ordering new ones would possibly have taken too long. Due to the way our hypothesis is formulated, this would not pose a significant problem.

The test plan is designed to answer how much changing the size of the propellers and the distance between them will impact efficiency and by extension how much additional flight time Nordic Unmanned would be able to achieve by implementing the findings on their Staaker BG200 drone.

Table 6.2: Test plan, Z_i for i = 0, 1, 2, 3, 4

Propeller A	Propeller B	Spacing
28"	28"	Z_i
30"	30"	Z_i
30"	28"	Z_i
32"	32"	Z_i
32"	30"	Z_i
32"	28"	Z_i

Table 6.2 and 6.3 shows how the testing is to be carried out, with the different propeller combinations and the different distances.

The Z values define the distance between the propellers. The Z-value is based on the

relationship of $Z_i = h/r_p$ where h is the distance between the propellers and r_p is the radius of propeller A. Both Q. Quan and F. Bohorquez is recommending a $h/r_p \geq 0.357$ [12, 15]. Table 6.3 shows that Z_2 is the optimal value according to Quan and Bohorquez´ testing, thus in order to have adequate coverage of both higher and lower values for Z_i with regards to Z_2 it was determined to have five different propeller distances with Z_2 being the middle value. Two extreme values, one being with the propellers as close as possible within reason and limitations of the test rig, and one being way larger. Z_1 is the propeller spacing Nordic Unmanned are currently using, and Z_3 being approximately equal to the difference Z_2 and Z_1.

Table 6.3: Propeller spacing

Z_i	0	1	2	3	4
H/R	0.14	0.31	0.36	0.48	0,65
28"	50mm	109mm	127mm	169mm	230mm
30"	53mm	109mm	136mm	182mm	246mm
32"	57mm	109mm	145mm	194mm	263mm

Determining what driving parameters would provide a clear indicator of how the efficiency changed, was not easy. Meaning, what kind of thrust range should be explored in the testing. This is due to the fact that accessing a log describing what loads the drone is experiencing, and how much thrust it produces throughout a regular operation, is difficult. In the first round of testing it was determined that exploring hover operation made the most sense, as logic states that a inspection/scanning drone would spend most of the time at hover. Thus a script for testing at hover thrust was written and testing was initialized.

Determining the thrust the Staaker BG200 needs to hover was done by investigating the maximum takeoff weight of the drone and dividing it by four, as the test rig represents 1 out of 4 coaxial arms.

$$T = \frac{1}{4}mg = 61.3N \tag{6.1}$$

It was also decided that in order to get good reliable data each test would be done three time and the results averaged. To avoid overheating and to get the most consistent performance

from the motors, a 2 minute pause was to be introduced between each test. The first batch of testing took about 6 hours effectively. The second batch of testing took about 10,5 hours, not considering setting the test up and changing of the test configuration. Last years thesis had a total of 26 successful tests. This is a relatively low number of tests when trying to improve such a system and get reliable data. Thus it was decided to increase this to 90 tests in addition to the 3 tests performed to calibrate the system.

7 Results

Efficiency is the key output used to calculate flight time. The point of this chapter is to present the results, then analyze the results in the discussion chapter.

The first sub chapter, calibrating test, is used to verify that the motor calibration is within acceptable ranges. The second sub chapter, Blade element momentum theory, tries to relate the theoretical BEMT model with the experimental data. The third sub chapter, Distances, is using the data from the figures 7.4-7.9 in combination with excel to calculate the change in percent from distance to distance. The fourth sub chapter, propeller sizing, is using the data from the figures 7.10-13 to create a table.

7.1 Calibration test

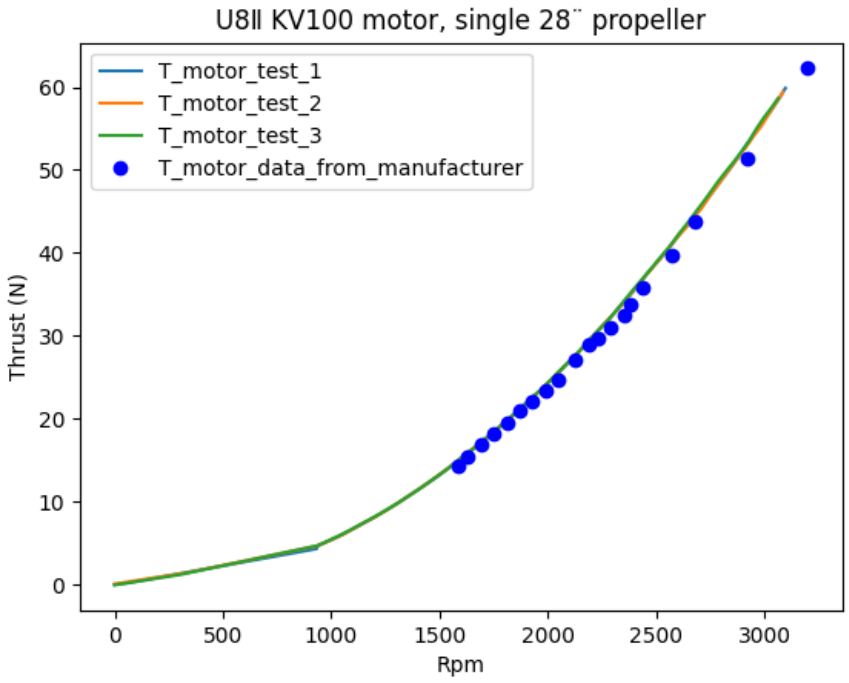

Figure 7.1: Calibration of T-motor U8II KV100

To verify the calibration of the test rig, the first test performed was a single 28"x9.2" propeller. The test data that are used in figure 7.1 comes from T-motors web page [19] and are compared with our experimental data. Our test data is coalescing with the manufacturers data, see figure 7.1, this verifies that the test rig is ready to use.

7.2 BEMT

As presented in the theory chapter, BEMT builds on splitting up the propellers into smaller parts and calculating the thrust and torque for each section. The plot resented has thrust on the y-axis and rpm on the x-axis. When including the other graphs for different distances, the result was that they had no significant difference in thrust against rpm.

After consulting Jørgen Apeland from Nordic Unmanned, it appeared that the same propeller on top and bottom was the most interesting, so modification of the pyBEMT script focused on creating inputs for 30U 30L and 32U 32L.

The airfoil inputs for the pyBEMT model for the 30U 30L and the 32U 32L has been borrowed from Adrian Otter Falch Günther´s master thesis [20]. The inputs for the that was required was chord, pitch, section type and radius. The outcome from these calculations are the dots in figure 7.2 represents the theoretical performance generated from the pyBEMT model [16, 17].

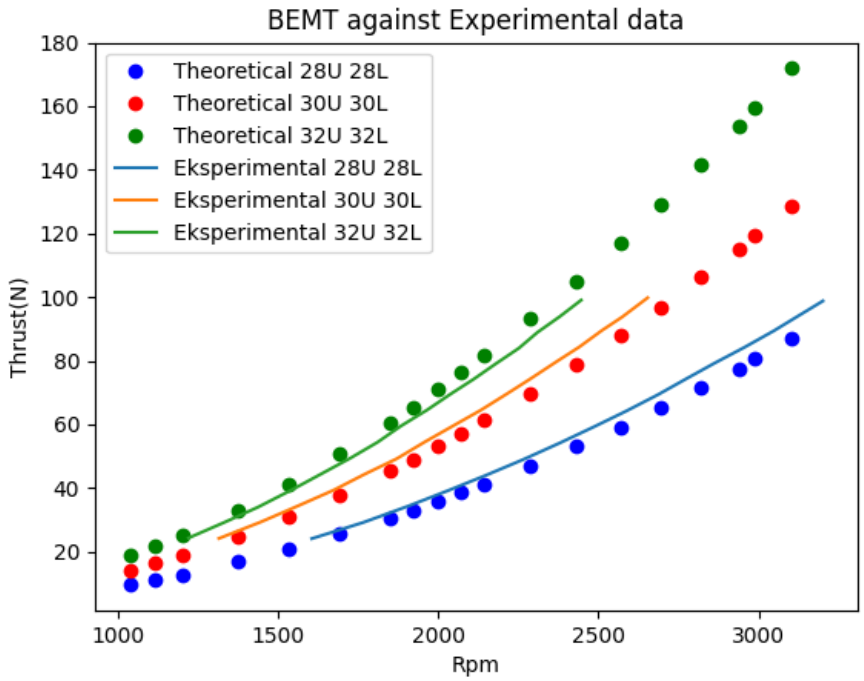

..

Figure 7.2: The Blade Element Momentum Theory

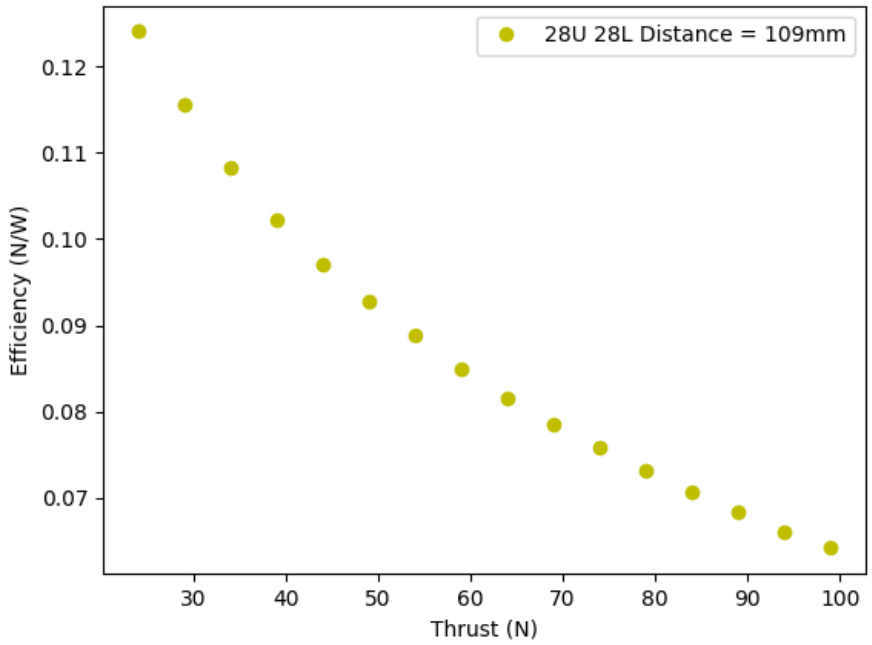

Figure 7.3: Thrust range efficiency

Figure 7.3 shows the thrust range with thrust on the x-axis and efficiency on the y-axis, and illustrates that the efficiency is reduced as thrust increases.

7.3 Propeller spacing

Figure 7.4 to 7.9 displays the efficiency against the distance between the propellers. These plots are created to show the thrust range of each propeller and how the distance between the propeller influence the efficiency. The thrust range explained earlier represent the efficiency at the different thrust values.

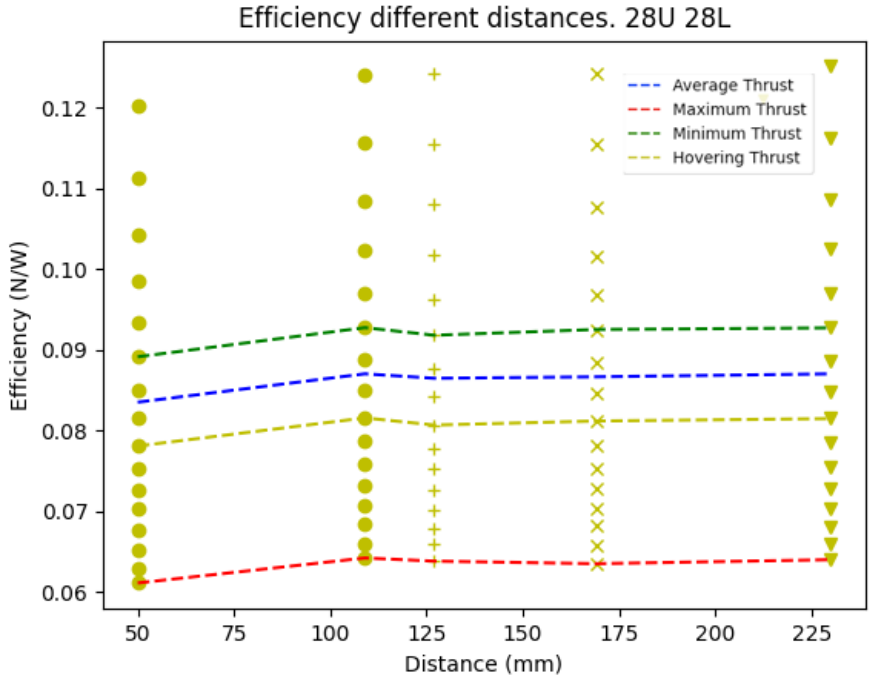

Figure 7.4: 28U 28L

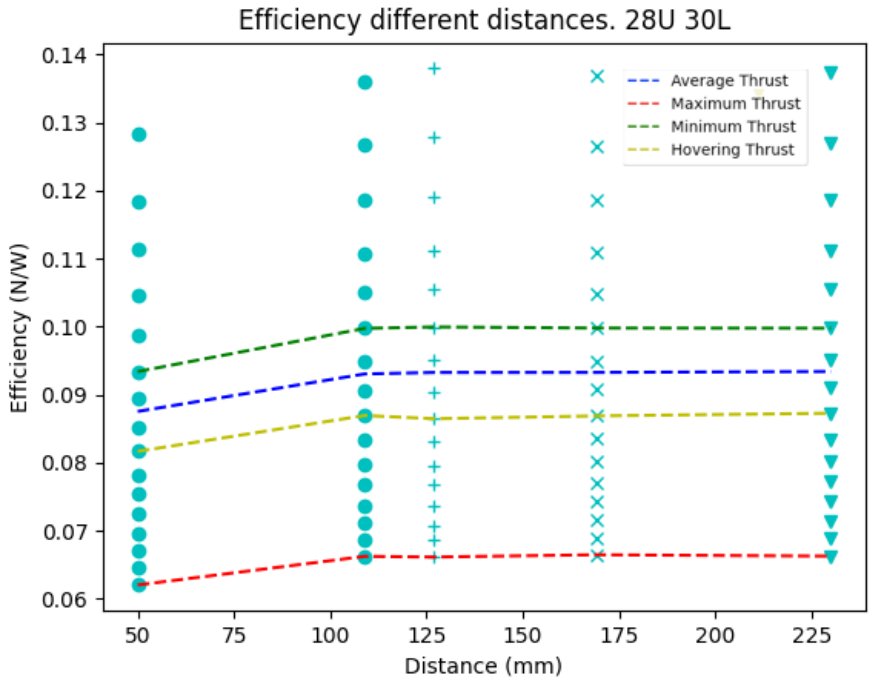

Figure 7.5: 28U 30L

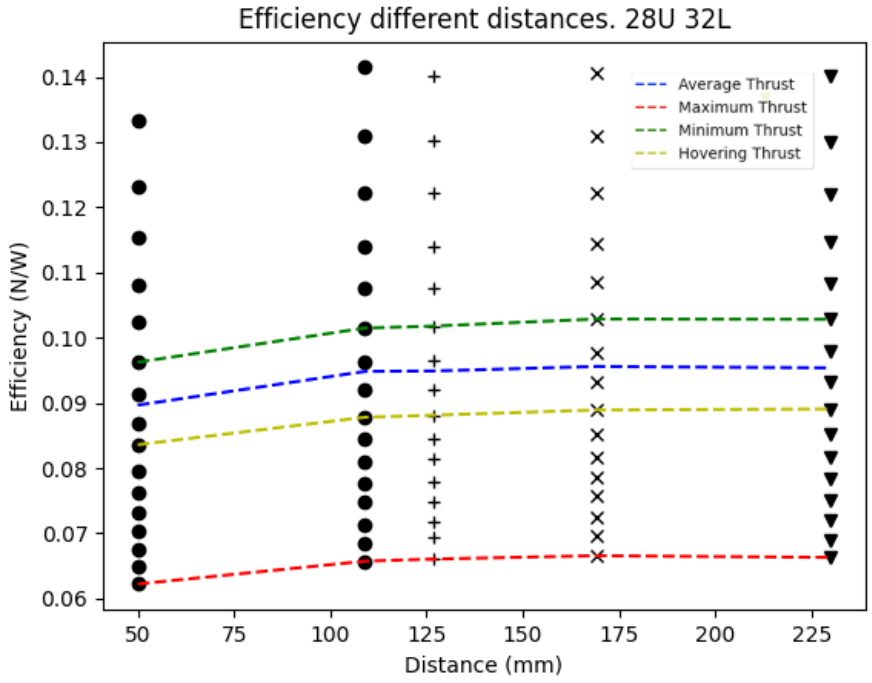

Figure 7.6: 28U 32L

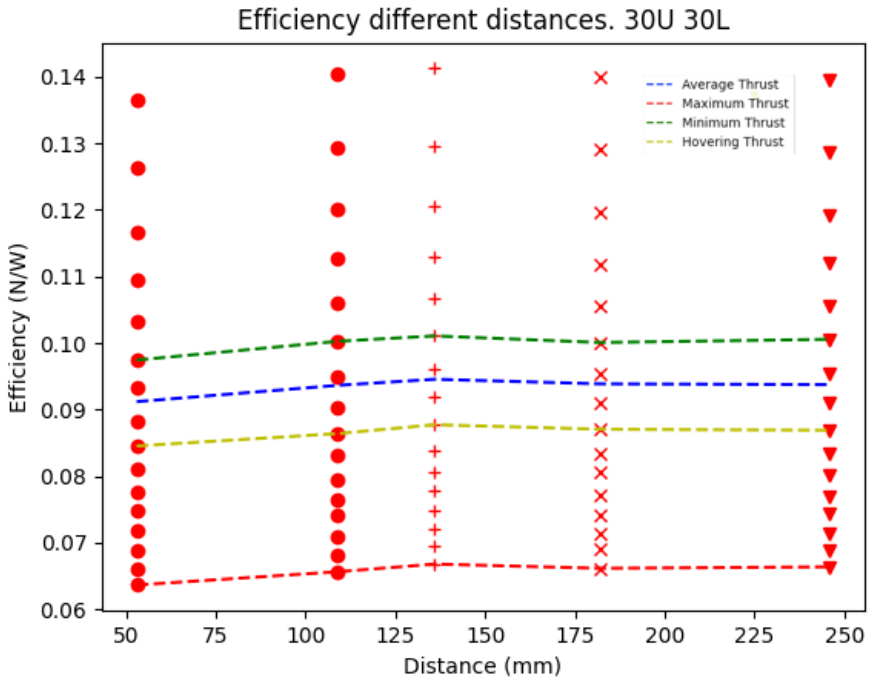

Figure 7.7: 30U 30L

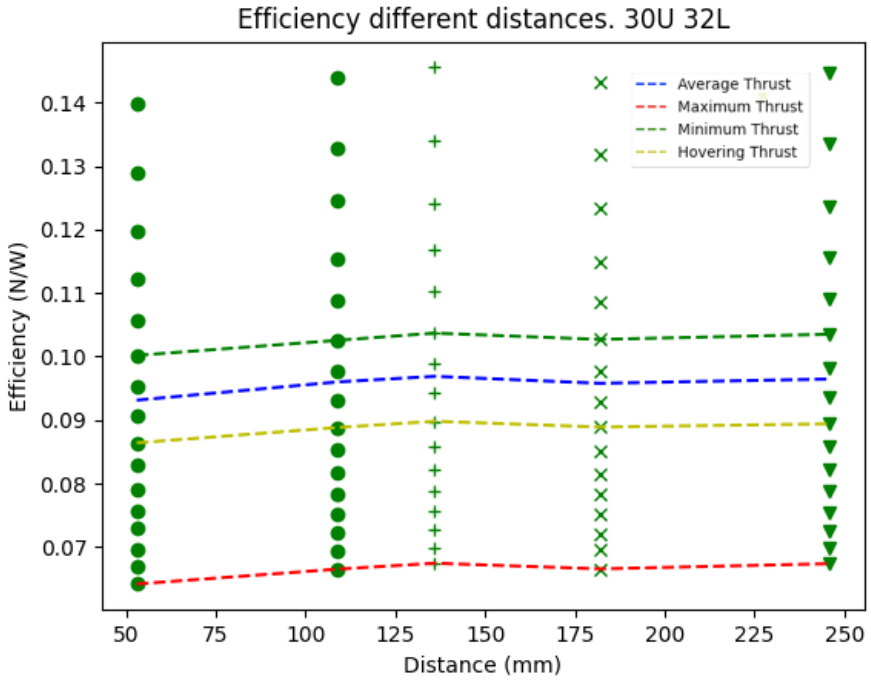

Figure 7.8: 30U 32L

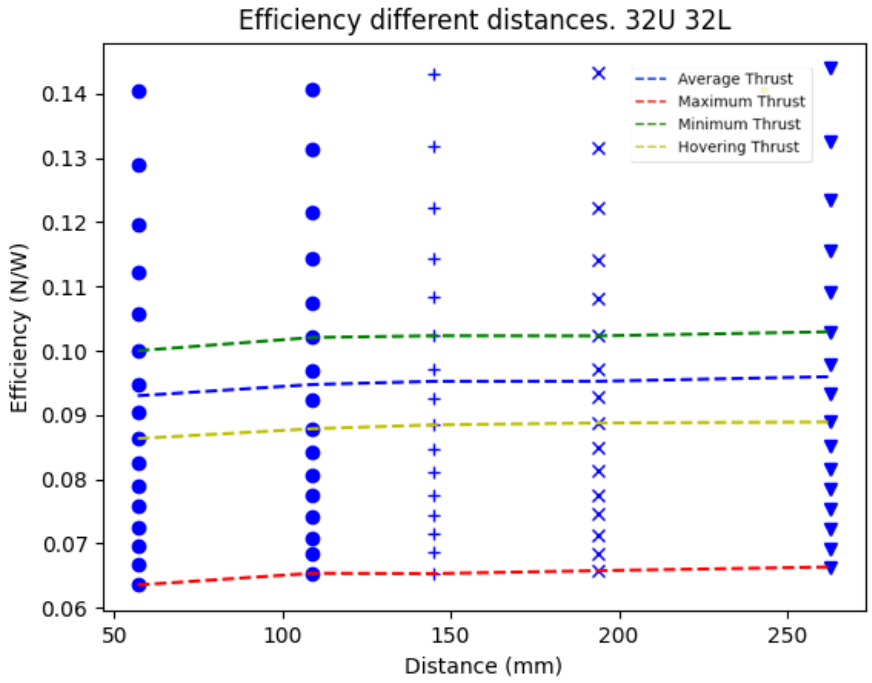

Figure 7.9: 32U 32L

Different experiments under four different scenarios were constructed to analyse the test data. The first scenario, hovering, is important to illustrate the energy used when hovering with a steady thrust. The second scenario, maximum thrust, is used to illustrate the energy when accelerating up. The third scenarios, minimum thrust, is used to illustrate the energy used when accelerating down. The last, average thrust, is the average of all the points in the thrust range and are useful in the scenario when accelerating a lot up and down. The dashed lines in figure 7.4 to 7.9 represents the different scenarios for the drone, and are used in later plots to compare different propellers in figure 7.10 to 7.13.

As mentioned earlier, the former hypothesis was that the optimal setup for Staaker BG200 was to have a small propeller on top and a larger as the lower, meaning in this case 28U 32L with a Z_4 distance between the propeller. Z_1 is the distance Nordic Unmanned are using today and equals 109.2 mm. Using Z_1 as a status quo distance to inspect how changing the distance changes the efficiency.

Table 7.1 shows the percentage change in effiency between the same configuration of propeller

when changing the distance. In the first row the distance changed from status quo to Z_0, and in the second row the distance are changed from statues quo to Z_4.

Table 7.1: Efficiency difference, changing distance

	28U 28L	28U 30L	28U 32L	30U 30L	30U 32L	32U 32L
$Z_0 - Z_1$	- 4,2%	- 6,3%	- 5,8%	- 3,1%	- 2,7%	- 1,9%
$Z_4 - Z_1$	0,0%	0,4%	0,6%	0,5%	0,1%	1,3%

Analysing plot 7.10-7.13 shows that there are sometimes a decrease in performance when increasing the space between the propellers. An example is from Z_1 to Z_2 for the 28U 28L, where an decrease in efficiency can be observed.

7.4 Propeller configuration

Figure 7.10 to 7.13 displays the efficiency between the different propeller configurations. The reasoning behind these plots was to make it possible to compare the different propellers on max, min, hovering and average. Table 7.2 shows the percentage efficiency difference when changing the configuration of the propellers, and tries to display the same information in figure 7.10 to 7.13 in a clear way. The data in this table was generated from the python script.

Table 7.2: Percent efficiency change for different propeller configurations

	Avg	Min	Max	Hovering
28U 30L	7,0 %	3,2 %	7,6 %	6,6 %
28U 32L	9,0 %	2,4 %	9,5 %	9,5 %
30U 30L	9,0 %	3,7 %	10,6 %	10,6 %
30U 32L	10,4 %	3,7 %	8,1 %	8,1 %
32U 32L	8,9 %	1,9 %	10,1 %	10,1 %

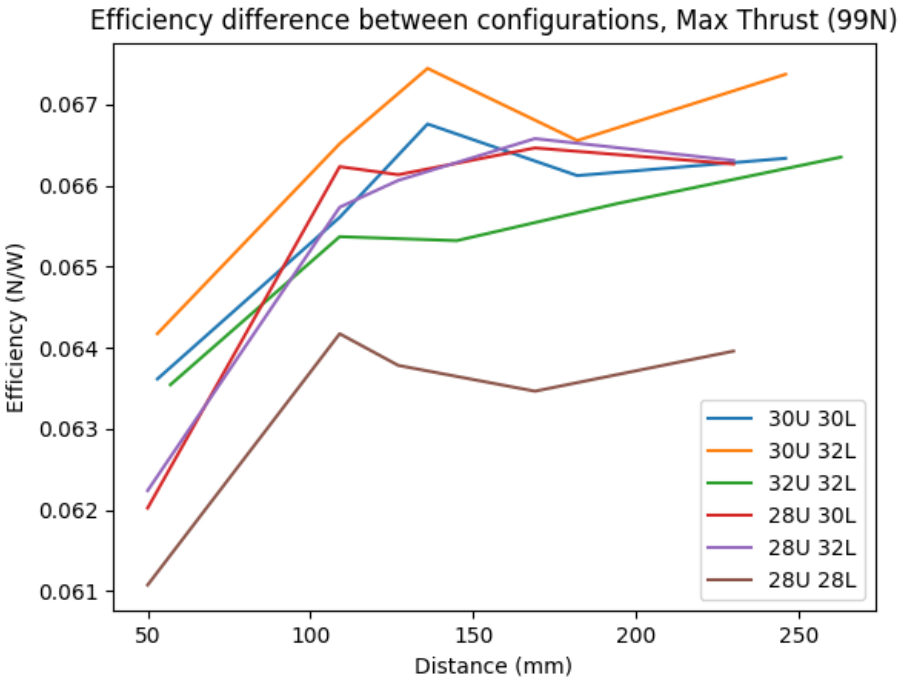

Figure 7.10: Maximum thrust

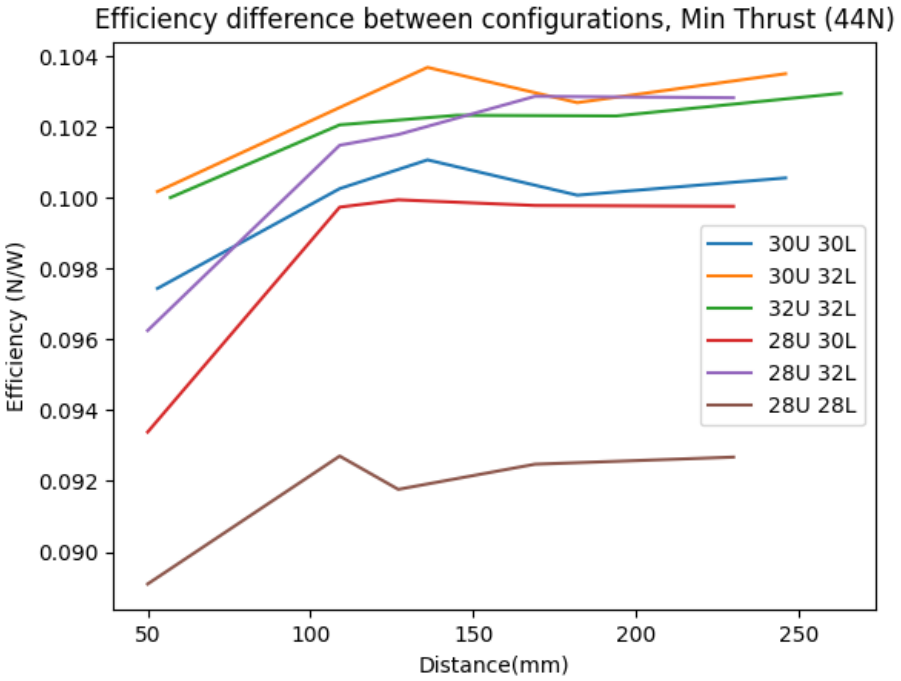

Figure 7.11: Minimum thrust

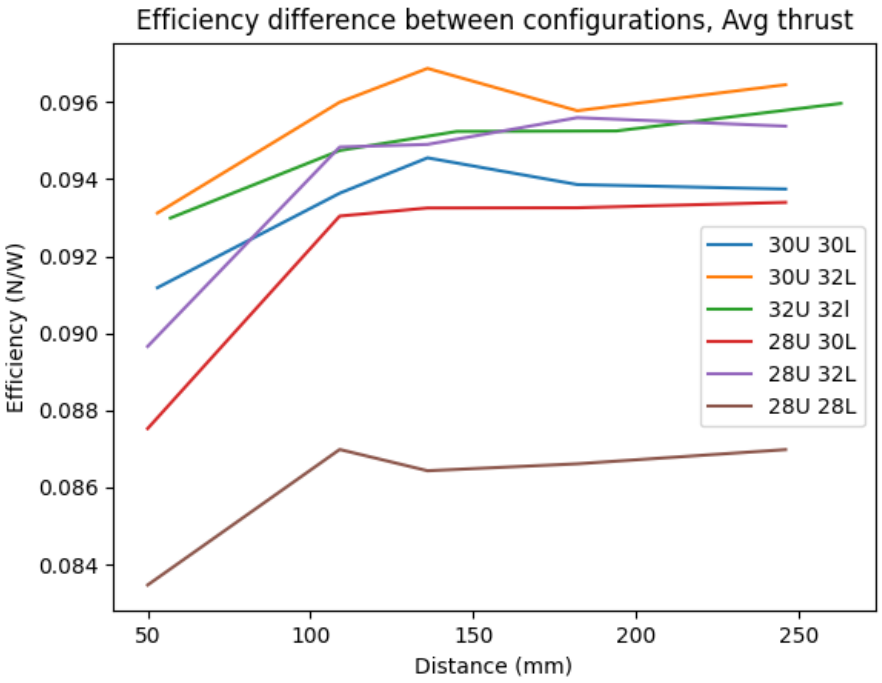

Figure 7.12: Average thrust

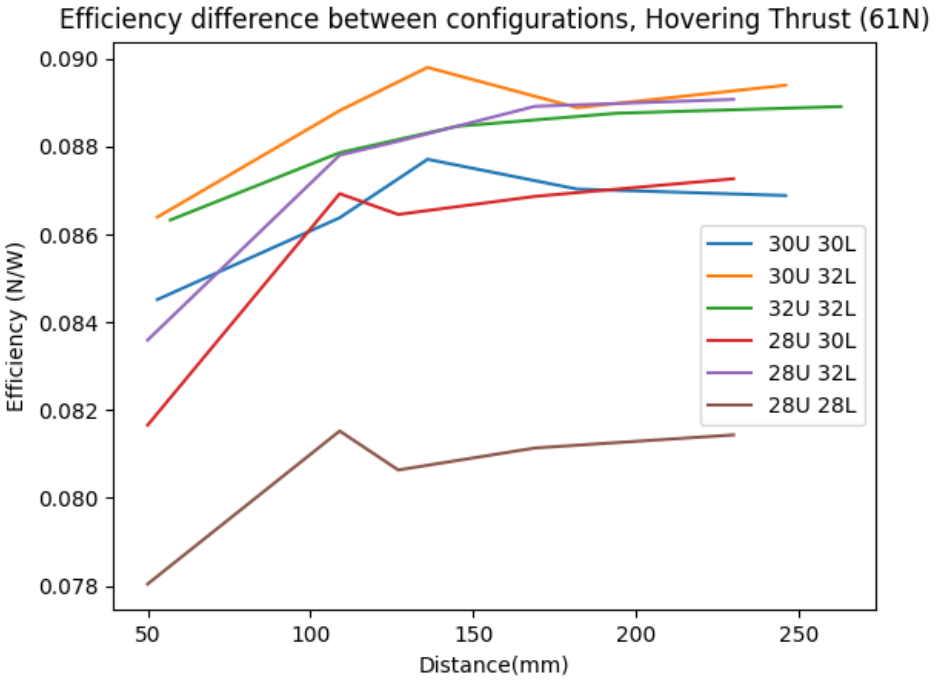

Figure 7.13: Hovering thrust

7.5 Optimizing the propeller

The method used to find the optimized propeller geometry is to use the pyBEMT script and iterate by increasing the input pitch. First case increasing the pitch for the hole blade, second case re-designing the blade by increasing the exposed areas.

The result is illustrated in figure 7.14, this shows that by changing the pitch by 1 the theoretical change of efficiency is 3.1 % for the thrust 92 Newton. Equation (7.1) shows how the change in efficiency is calculated. 3.1 % equals aproximatly 1.55 % for the total system.

$$\Delta Efficiency = \frac{0,0844 - 0,0815}{0,0815} = 0,031 \tag{7.1}$$

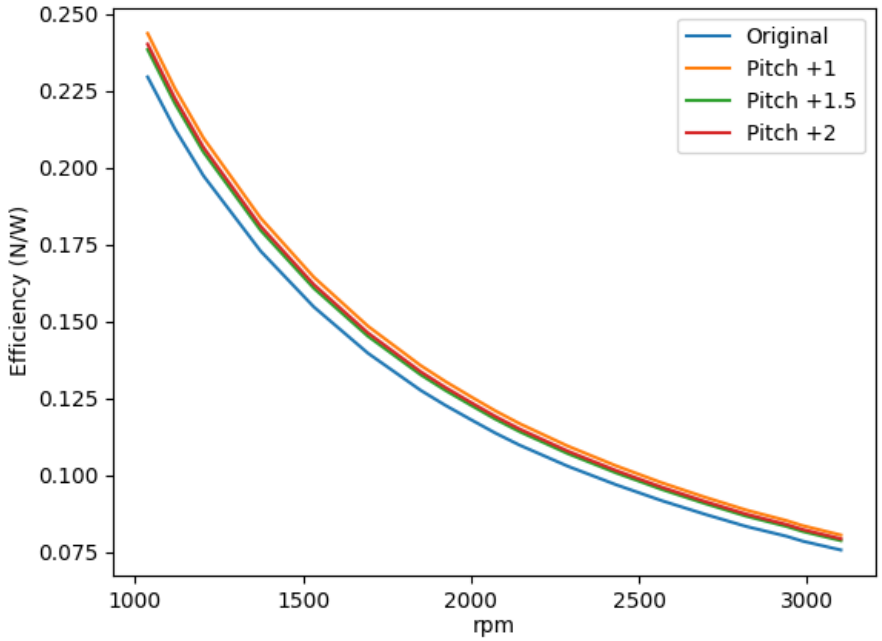

Figure 7.14: Optimizing for angle of attack

Second case should be the most optimal way, for the two scenarios, to improve the efficiency. Change the pitch for the sections that are exposed to the air exhaust from the upper propeller. Using the pyBEMT script to create one graph with the pitch changed for the entire blade and

one graph where the pitch was changed for the sections exposed to the exhaust air particles illustrated in figure 7.15. In this the label pitch +1 inside means changing the pitch of the blade section inside the exposed particles. In pyBEMT one of the criteria is that the lower propeller has to be in the fully developed slipstream, this means that there are 7 sections in the slipstream and 3 sections not exposed.

In figure 7.15 the graph of pitch +1 inside and pitch +1 is almost equal, this is a result of that the thrust is generated from the inner sections. In other words, the efficiency is mostly influenced by the sections closest to center.

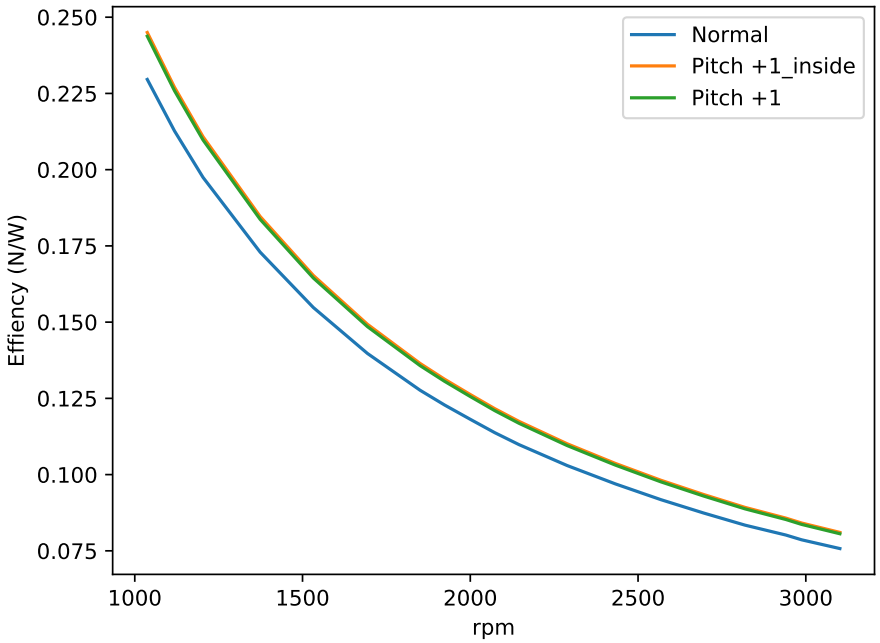

Figure 7.15: Optimizing for angle of attack for pitch inside the exhaust area

8 Discussion

Our former hypothesis was that a small propeller in front and a larger propeller in back with an as large as possible distance in between, within reasonable distance, would give the optimal efficiency. The results focusing on distance indicates that the critical point has been reached when the distance that Nordic unmanned are using now for all the propeller. The results focusing on propeller configuration indicates that the optimal configuration when taking into consideration variables as maneuvering and how the drone would react to different propellers is 30U 30L.

8.1 Propeller spacing

The results from table 7.1 is in correlation with Quan [15] experimental findings, that ($h/r_p \geq 0.357$) which represent Z_2 in this systems. The reasoning behind using $Z_1(109mm)$ as status quo, is that this distance is the same as Nordic Unmanned uses on their Staaker BG200.

Two scenarios were analyzed. The first scenario is when the distances are extended past the status quo, illustrated in column two in table 7.1. The second scenario is when the distance is closer together than the statues quo, shown in column 1 in table 7.1.

Inspecting table 7.1 the first scenario indicates, that flight time will not improve more than 1.3 % by extending the distance from Z_1 to Z_4 for 32" propeller in upper position. Also, the efficiency will not improve more then 0.6 % by extending the distance from Z_1 to Z_4 for the 28" propeller in the upper position. Additionally, the efficiency will not improve more than 0.5 % when the distance is changed from from Z_1 to Z_4 for 30" propeller in the upper propeller.

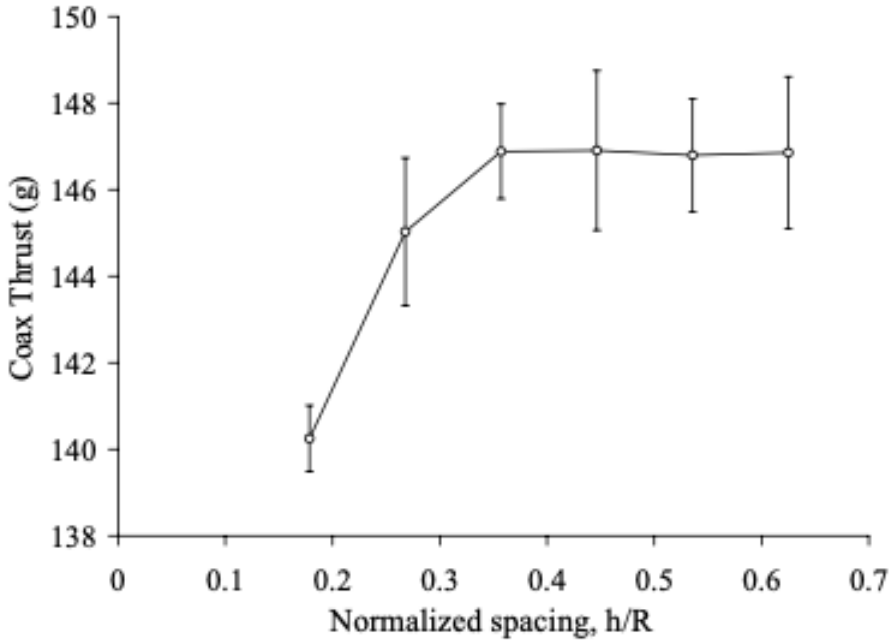

Figure 8.1: Coaxial performance with 2500 rpm [12]

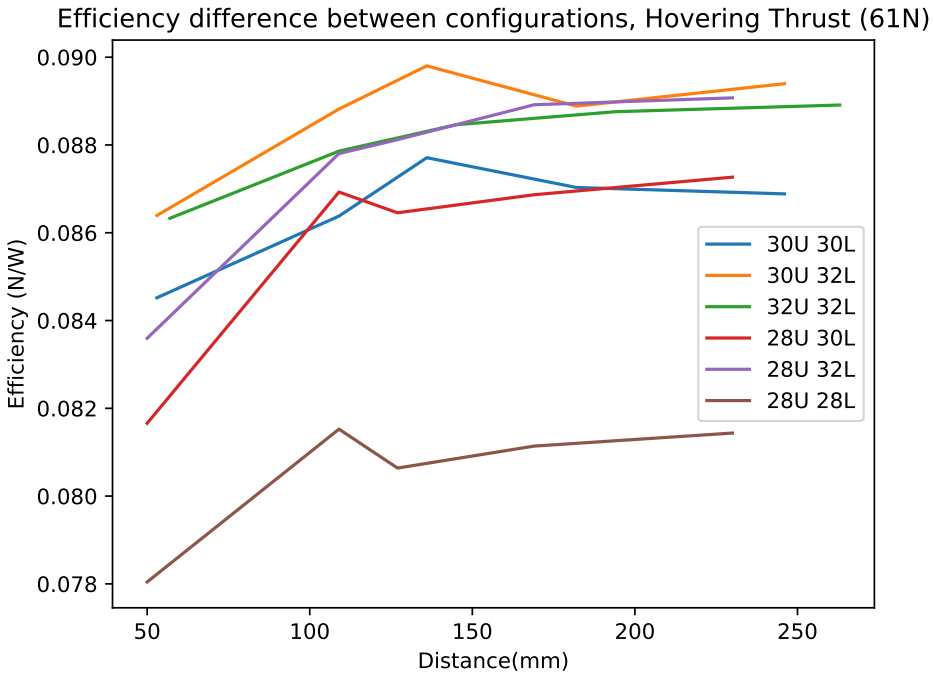

Figure 8.2: Hovering Thrust

In the second scenario, spacing of the propeller is smaller than statues quo. Table 7.1 column

two, shows that for every configuration from 1.9 % to 6.3 % decrease in efficiency. This indicates that decreasing distance between the propellers gives a major decrease in efficiency. This data correlate with Q. Quan and F. Bohorquez [15, 12], and having the propellers closer together than ($h/r_p \geq 0.357$) decreases efficiency. By comparing (Figure 8.1 and 8.2), the correlation is significant, although Bohorquez uses thrust and this thesis uses efficiency on the y-axis. This shows that when exceeding the distance of ($h/r_p = 0.357$), Z_2 in our model, the efficiency is not significantly influenced.

Looking back on the hypothesis with the new information accumulated through articles and analysis. The results would change the hypothesis by stating that the distance Z_2 ($h/r_p \geq 0.357$) is optimal. Although Q. Quans study uses smaller propellers than us, which means lower Reynolds numbers, his experimental data overlaps our data.

In practical terms this means that the influence of spacing between the propellers, results in the conclusion that the spacing Nordic unmanned uses today is sufficient. Although increasing the distance to ($h/r_p = 0.357$) could lead to 1 % increase in efficiency. This gain is minor, therefore changing the current propellers distance will result in minor improvements compared to the possible economical cost of implementing. This makes it not worth the change. Consulting Nordic Unmanned for the percentage they would consider changing the distance for, their response was 5 %, and is lower than the experimental data.

8.2 Propeller configuration

From the chapter 8.1 our conclusion was that the distance $Z_1(109mm)$ was sufficient for Nordic Unmanned, this is why from this point on the analysis only uses the size $Z_1(109mm)$.

In results data from figure 7.10-7.13 are used to calculate the percentage change in table 7.2. This table displays the percentage change from the status quo configuration to different configurations, with the four different scenarios explained in the result chapter. Directly from inspecting the plots 7.10-7.13, one can see that 28U 28L is not an energy efficient configuration of propellers, compared with other configurations. This correlates with the blade element model figure 7.2, but the gap between the efficiency was larger than expected.

This also matches the literature from C. Simoes [13]. He stated "The results have shown that propellers with a larger diameter were typically more efficient". This matches the test data for 28" to 30" propeller, but for the 32" propeller it was almost the same efficient than 30" propeller. Our hypothesis, is that U8II KV100 is not powerful enough for the 32", and further work should investigate this.

From inspecting table 7.2 the highest change for the thrust range percent on average was with the configuration 30U 32, and had an increase of 10.4 %. Average for the thrust range is arguable a good variable when considering flight time, because drones accelerate up and down. The hovering scenario can be just as good of a data set as average, because these drones are mostly used for long distance mapping of areas. Hovering means that the drone have a steady speed in one direction and do not accelerate up and down. As well as taking into consideration that our contact person from Nordic Unmanned, Jørgen Apeland, informed us that it is a bigger step adjusting the drone for larger propellers. Additionally, he explained that the maneuvering capacity is unknown when using different blades. Therefore our recommendations for propeller configuration is to switch from 28U 28L to 30U 30L. This gives a 10.6 % increase with steady speed and 9 % increase for the thrust range, at least when using the test rig. The implication for Nordic Unmanned is that if they decide to follow our recommendations, they need to extend the arms and the electrical cables inside the arms.

8.3 Flight time

$$Flighttime = \frac{Energy}{Power} = \frac{Energy}{\frac{Gravity * Mass}{Prop.eff}} \tag{8.1}$$

This section will present flight time using data from the experiments focusing on the propeller combination that gave us the highest efficiency($t_{new} = 30U30L$) against the propeller Nordic unmanned uses today($t_{old} = 28U28L$). First of all, taking a deeper dive into the thrust range from 20 % to 80 % and using the efficiency from the average of the thrust range.

Equation (8.1) is used to calculate the flight time, by using energy consumed divided by the power produced for the drone. This equation uses 80 % of the battery capacity, because 20 %

needs to be in backup for the landing maneuver. This means that the usable energy for the drone equals 1208 watt hours. Mass depends on the drones weight for the scenario in regards to which battery configuration is being used and payload. Propeller efficiency is calculated using the thrust in Newton divided on the electrical power consumption for the drone. These numbers are derived from the CSV files, found in attachments.

Table 8.1 is the resulting propeller efficiency and the flight time for the drone operating in the thrust range with and without payload. Table 8.2 is the resulting propeller efficiency and the flight time for the drone operating in the hovering scenario with and without payload. These two tables shows that changing the propeller configuration will give a significant improvement.

Table 8.1: Thrust range from 20% to 80% scenario

	Propeller effi	Mass	Flight time
t_{old}	0,0870	25kg	25,71 min
t_{new}	0,0948	25kg	28,02 min
t_{old}	0,0870	18,6kg	34,56 min
t_{new}	0,0948	18,6kg	38,76 min

Table 8.2: Hovering scenario

	Propeller effi	Drone Weight	Flight time
t_{old}	0,0848	24,3kg	25,78 min
t_{new}	0,0937	24,2kg	28,51 min
t_{old}	0,0975	17,9kg	40,24 min
t_{new}	0,0110	18kg	45,15 min

8.4 Possible sources of error:

As a result of how the experiment is designed and limitations in tools and expertise there are a couple of possible sources of error through the experiment. As far as how much of an impact these possible errors have on the final results is hard to estimate.

The propellers has been connected to the motors by utilizing T-motors quick connectors 26”-34”. During testing a development of a slop was noticed. These quick connections are the same that has been used by earlier groups in testing. Determining if the slop is inherent to the design, if it comes from excessive wear of is a product fault is hard to determine. Nordic

Unmanned has been informed about this development, and are considering replacing them for further testing.

To measure the distance between the propellers, a digital caliper was used. To establish the Z_1, which is the zero-point, or in other words the spacing Nordic Unmanned are using now, which is 109.2 mm, a string was used. The zero-point was hard to measure with a calipers. When this Z_1 was defined it was possible to establish a measurement between the base plates. The zero-point was hard to measure and is therefore a source of error.

As stated earlier, the motors used are the T-motor U8II KV100, which the manufacturer states are optimized for 27"-30" propellers [19]. Thus using the setup with the 32" propellers may have strained the motors more than they are able to handle and this could have impacted both the operational temperature and the efficiency of the setup. In the experiments there was not a temperature gauge. As a consequence to help combat possible overheating issues the decision to implement a 2 minute wait time between each run was done.

During the testing, instances of high vibration was occurred in the pillars of the test rig. The vibrations were mostly occurring during certain loads, about 20-25 N of thrust, and disappeared as the propellers continued the ramping towards full load. Some of the fasteners on the test rig had started to back out and thus re-tightened the loose fasteners and double checked all the bolts. This eliminated the vibration issues, which might be an effect of the loads coalescing with the rigs eigenfrequency, or normal frequency. To counteract the effect on the experimental data, some of the tests had to be redone.

The behaviour that some of the graphs goes down when increasing the distance, in figures 7.10-3.13, is a strange behaviour. In the perfect theoretical scenario the plots should be perfectly straight after reaching the critical point, like F. Bohorquez experiment illustrated in figure 8.1. The behaviour that the efficiency goes down is not identified, this could be because of failure in operation of the test rig. Three examples of the failures could be not torquing up the bolts on the quick connection correctly, not giving the motor enough rest time between tests or not torquing the bolts on the test rig correctly. It needs to be said that the drop is not large and the thesis group still regards the test results as valid.

8.5 Future work

Further work should consider changing the T-motor UII KV100 to larger ones. As mentioned earlier, T-motor states that the motor is optimal for 27"-30". This may lead to a greater efficiency for the 32" propeller. As well as counteracting the heat development occurring during the testing.

If Nordic Unmanned decides to change their configuration to a larger propeller, the heat development may become a limiting factor. This should be considered for further investigations. For further testing heat sensors should be in place to investigate how much heat is developed and how it influences the efficiency of the motors.

Continue looking into the propeller itself would also be interesting. Either by testing different pitches like C. Simoes did in his article [13], or going deeper into the blade element momentum theory and investigating the optimal combination of chord and pitch. As well as including wind into the system with the pyBEMT model or wind tunnel testing would be interesting.

8.6 Recommendations

The goal from Nordic Unmanned for the thesis was clear. They wanted specific recommendations with theory and numbers backing the recommendations.

The recommendations from this work is that Nordic Unmanned should not change the distance between the propellers, because of the possible economical cost and the unknown consequences will probably not outweigh the benefit of getting approximately 1 % increase in the flight time. But they should consider changing the propeller configuration to a 30U 30L propeller size. This should, from experimental data collected, give an increase of 10.6 % when hovering and 9.0 % when accelerating, compared to the propeller configuration Nordic Unmanned are using today.

9 Conclusion

The research aimed to identify what would give Nordic unmanned the longest flight time, by finding the distance and configurations between two propellers operating in a coaxial system. Based on literature, information from Nordic Unmanned, past years bachelor and master thesis a test plan on how to find the most efficient propeller configuration was formulated. The theoretical and experimental results indicates that the optimal distance between the propellers, ranging from 28" to 32" propellers, is $h/r_p \geq 0.357$. Specifically for Nordic Unmanned they should keep the same distance as they have today. Since the distance they are using today are close to $h/r_p \geq 0.357$, and the possible cost will probably not outweigh the benefits.

Based on the information from calculating the change in the result section. Our recommendation is that Nordic Unmanned should consider changing configuration to 30U 30L, which gives an increase of 10.6 % when hovering and 9.0 % when accelerating. The reasoning behind this recommendation is that the hovering scenario matched what the drone normally are used for. As well as taking into consideration variables as maneuverability, going for a configuration of two different blades, and the amount of modifications needed to use this configuration.

The approach of trying to use blade element momentum theory to displayed that the the efficiency of the mechanical power would be greatest for the larger propeller sizes. Then analyse experimental data giving Nordic Unmanned their desired outcome gave a good results, and matched the literature for smaller propeller with smaller Reynolds numbers. This thesis may have filled some of the gap for propeller sizing, as was the goal in the literature study.

References

[1] E. Tandberg and Y. Jarslett. (2020) Drone. [Online]. Available: https://snl.no/drone, (visited_on_16/02/2021)

[2] Amazon. (2021) Amazon prime air. [Online]. Available: https://www.amazon.com/Amazon-Prime-Air/b?ie=UTF8&node=8037720011.(visited_on_16/02/2021)

[3] IKM. (2020) Ikm inspection drones. [Online]. Available: https://www.ikm.no/ikm-testing/utstyrskatalog/uav-droner.(visited_on_16/02/2021)

[4] N. Unmanned. (2020) Nordic unmanned business operations. [Online]. Available: https://nordicunmanned.com/business-areas.(visited_on_16/02/2021)

[5] N. Unmanned. (2020) Nordic unmanned business operations. [Online]. Available: https://nordicunmanned.com/business-areas.(visited_on_16/02/2021)

[6] T. Robotics. (2020) Series 1780 25 40 kg dynamometer user manual v2.5, no. cxh29d. [Online]. Available: https://cdn-docs.rcbenchmark.com/manuals/series-1780/Series%201780%20v2.5%20General%20User%20Manual.pdf,(visited_on_10/02/2021)

[7] S. R. Hidle and V. B. Ingebretsen, "Improvement of effeiciency of a coaxial octodrone," Bachelor in Maskin ingeniør, Det Teknisk-Naturvitenskapelige Fakultet, Universitet i Stavanger, Stavanger, 2020.

[8] J. F. Manwell, J. G. McGowan, and A. L. Rogers, *Aerodynamic of Wind Turbines", Wind energy explained: theory, design and application.* John Wiley & Sons, 2nd ed, West Sussex, United Kingdom, 2009, p.92-129.

[9] S. D. Prior, *Optimizing small multi-rotor unmanned aircraft: A practical design guide.* CRC Press, 1nd ed, london, United Kingdom, 2018, pp. 59-64.

[10] N. G. R. Center. (2014) Reynolds number. [Online]. Available: https://www.grc.nasa.gov/www/BGH/reynolds.html.(visited_on_05/02/2021)

[11] R. W. Deters, G. K. Ananda, and M. S. Selig, "Reynolds number effects on the performance of small-scale propellers," *AIAA Aviation*, pp. 1–39, 2014, Available: https://m-selig.ae.illinois.edu/pubs/DetersAnandaSelig-2014-AIAA-2014-2151.pdf?fbclid=IwAR3ZXZDBg5G2mQTQd7pq6XmC9vTYJSHO8ljsd8humXk12YCioBQYZK8MJpY.

[12] F. Bohorquez, "Rotor hover performance and system design of an efficient coaxial rotary wing micro air vehicle," Doctoral dissertation in Aerospace Engineering, University of Maryland, College Park, 2007.

[13] C. Simoes, "Optimizing a coaxial propulsion system to a quadcopter," pp. 4–9, 2016, Available: https://fenix.tecnico.ulisboa.pt/downloadFile/563345090412782/Resumo.pdf.

[14] J. G. Leishman and S. Ananthan, "Aerodynamic optimization of a coaxial proprotor," in *Annual Forum Proceedings-American Helicopter Society*, vol. 62, no. 1. American Helicopter Society, INC, 2006, pp. 2–8, DOI: 10.4050/JAHS.57.042 003.

[15] Q. Quan, *"Airframe Design," Introduction to multicopter design and control.* Springer, Singapore, Malaysia, 2017, p.60.

[16] K. E. T. Giljarhus. (2020) pyBEMT. [Online]. Available: https://github.com/kegiljarhus/pyBEMT.(visited_on_04/06/2021)

[17] K. E. T. Giljarhus, "pyBEMT: An implementation of the blade element momentum theory in python," *Journal of Open Source Software*, vol. 5, no. 53, p. 2480, 2020, Available: https://joss.theoj.org/papers/10.21105/joss.02480.

[18] Creaform/Metek. (2017) Handyscan 700 specifications. [Online]. Available: https://www.creaform3d.com/sites/default/files/assets/brochures/files/handyscan3d_brochure_en_hq_21032017_2.pdf,(visited_on_15/03/2021)

[19] T-Motor. (2020) T-motor u8 ii kv100. [Online]. Available: https://store-en.tmotor.com/goods.php?id=561.(visited_on_04/06/2021)

[20] A. O. F. Günther, "Co-axial propeller configuration optimization," Master dissertation in Mechanical and Structural Engineering and Material, Faculty of Science and Technology, University of Stavanger, 2020.

Appendix

Appendix A is the standard script that is used to read the CSV-file and create four lists Thrust A, Thrust B, Power A and Power B. Using these four lists to calculate the efficiency from one test. The script performs this process three times, to include all the tests performed on the same propeller configuration and distance.

After having the raw data in lists, the script iterates threw the efficiency lists and records the efficiency at minimum, maximum and hovering. As well as calculating the average of the thrust range, returning the information for later scripts to plot.

Appendix B is the script that created the plot in figure 7.7. The script imports the data from appendix A and four other similar scripts. Then collecting the different propeller spacing in the same plot.

Appendix C is the script that was used to run the RCbenchmark test rig, and was explained in sub chapter 6.3.

A Example python script for reading CSV-file

```
import pandas as pd
import matplotlib.pyplot as pl
import numpy as np



class Z1_Thirty_Thirty_Thrust:
    def reading_test_1(self):
        #Finds the CSV-file
        self.df = pd.read_csv("/Users/sondregysland/PycharmProjects/"
                              "pythonProject/Batchlor_Ny/"
                              "Data_fra_testing"
                              "/Z1_Thirty_Thirty_Thrust/"
                              "30x30_Z1_test_3_2021-03-03_153009.csv"
                              , delimiter=',')
        #Reads the specific row.
        Thrust_A = self.df["Thrust A (N)"]
        Power_A = self.df["Electrical Power A (W)"]
        Thrust_B = self.df["Thrust B (N)"]
        Power_B = self.df["Electrical Power B (W)"]
        #Adds the thrust/power togheter,
        # to find the totall thrust/power.
        Ptot = np.add(Power_A,Power_B)
        Ttot = np.add(Thrust_A,Thrust_B)
        #Calculates the effiency
        Reation = Ttot/Ptot
        return Reation
```

```
def reading_test_2(self):
    df = pd.read_csv("/Users/sondregysland/PycharmProjects/"
                     "pythonProject/Batchlor_Ny/"
                     "Data_fra_testing/"
                     "Z1_Thirty_Thirty_Thrust/"
                     "30x30_Z1_test_2_2021-03-03_151241.csv"
                     , delimiter=',')
    Thrust_A = df["Thrust A (N)"]
    Power_A = df["Electrical Power A (W)"]
    Thrust_B = df["Thrust B (N)"]
    Power_B = df["Electrical Power B (W)"]
    Ptot = np.add(Power_A,Power_B)
    Ttot = np.add(Thrust_A,Thrust_B)
    Reation = Ttot/Ptot
    return Reation


def reading_test_3(self):
    df = pd.read_csv("/Users/sondregysland/PycharmProjects/"
                     "pythonProject/Batchlor_Ny/"
                     "Data_fra_testing/"
                     "Z1_Thirty_Thirty_Thrust/"
                     "30x30_Z1_test_3_2021-03-03_153009.csv"
                     , delimiter=',')
    Thrust_A = df["Thrust A (N)"]
    Power_A = df["Electrical Power A (W)"]
    Thrust_B = df["Thrust B (N)"]
    Power_B = df["Electrical Power B (W)"]
    Ptot = np.add(Power_A,Power_B)
```

```
        Ttot = np.add(Thrust_A,Thrust_B)
        Reation = Ttot/Ptot
        return Reation

    def Beskriveles(self):
        #Runes the reading function.
        P1 = self.reading_test_1()
        P2 = self.reading_test_2()
        P3 = self.reading_test_3()
        #Adds the tree tests together.
        P = np.add(P1,P2)
        P_p = (np.add(P,P3))/3
        x = [109] * len(P_p)
        #Plots 109mm on the x-axis
        # and Efficiency on the y-axis.
        pl.plot(x,P_p, "ro")
        return P_p

    def Avg(self):
        #Runes the reading function.
        P1 = self.reading_test_1()
        P2 = self.reading_test_2()
        P3 = self.reading_test_3()
        #Adds the tree tests together.
        P = np.add(P1,P2)
        P_p = (np.add(P,P3))/3
        Avg = 0
        #Iterates threw the list
        # and takes the average.
        for i in P_p:
```

```
            Avg += i
        Verdi = Avg/16
        return Verdi


def Running_program(self):
    self.Beskriveles()

def Maks(self):
    #Runes the reading function.
    P1 = self.reading_test_1()
    P2 = self.reading_test_2()
    P3 = self.reading_test_3()
    #Adds the tree tests together.
    P = np.add(P1,P2)
    P_p = (np.add(P,P3))/3
    y = 0
    #Iterates threw the list and extract
    #line number 15,
    # which represent 94N
    # and Nordic mans max thrust.
    for i in P_p:
        if y == 15:
            Maks = i
        y += 1
    return Maks
```

```
def Min(self):
    #Runes the reading function.
    P1 = self.reading_test_1()
    P2 = self.reading_test_2()
    P3 = self.reading_test_3()
    #Adds the tree tests together.
    P = np.add(P1,P2)
    P_p = (np.add(P,P3))/3
    y = 0
    #Iterates threw the list and extract
    #line number 5, which represent 39N
    # and Nordic mans Min thrust.
    for i in P_p:
        if y == 5:
            Min = i
        y += 1
    return Min

def Take_off(self):
    #Runes the reading function.
    P1 = self.reading_test_1()
    P2 = self.reading_test_2()
    P3 = self.reading_test_3()
    #Adds the tree tests together.
    P = np.add(P1,P2)
    P_p = (np.add(P,P3))/3
    y = 0
    #Iterates threw the list and extract
    #line number 8, which represents 61N
    # and Nordic mans take off thrust.
```

```
        for i in P_p:
            if y == 8:
                Take_off = i
            y += 1
        return Take_off

    def Min_Take_off_Maks(self):
        #Runs the function min maks and avg.
        self.Min()
        self.Take_off()
        self.Maks()
```

B Example python script importing and plotting data

```
import matplotlib.pyplot as pl

#Imports the 30U" 30L" propellers Z0,Z1,Z2,Z3 and Z4
import Batchlor_Ny.Data_fra_testing.Z0_Thirty_Thirty_Thrust.\
    Z0_Thirty_Thrity_Thrust2 as Sicks
import Batchlor_Ny.Data_fra_testing.Z1_Thirty_Thirty_Thrust.\
    Z1_Thirty_Thrity_Thrust2 as One
import Batchlor_Ny.Data_fra_testing.Z2_Thirty_Thirty_Thrust.\
    Z2_Thity_Thity_Thrust2 as Two
import Batchlor_Ny.Data_fra_testing.Z3_Thirty_Thirty_Thrust.\
    Z3_Thirty_Thirty_Thrust2 as Three
import Batchlor_Ny.Data_fra_testing.Z4_Thirty_Thirty_Thrust.\
    Z4_Thirty_Thirty_Thrust2 as Four
```

```
#Runs the function inside the imported scripts.
#Plots the given X-values(53,109,136,182,246mm)
#and the imported values on the Y-axis as points.
sicks = Sicks.Z1_Thirty_Thirty_Thrust()
sicks.Running_program()

Sicks_1 = Sicks.Z1_Thirty_Thirty_Thrust()
Seks = Sicks_1.Avg()

one = One.Z1_Thirty_Thirty_Thrust()
one.Running_program()

One_1 = One.Z1_Thirty_Thirty_Thrust()
Ein = One_1.Avg()

two = Two.Z2_Thirty_Thirty_Thrust()
two.Running_program()

#Plots the given X-values(53,109,136,182,246mm)
#and the imported average values on the Y-axis.
Two_2 = Two.Z2_Thirty_Thirty_Thrust()
To = Two_2.Avg()

three = Three.Z2_Thirty_Thirty_Thrust()
three.Running_program()

Three_1 = Three.Z2_Thirty_Thirty_Thrust()
Tri = Three_1.Avg()

four = Four.Z2_Thirty_Thirty_Thrust()
```

```
four.Running_program()

Four_1 = Four.Z2_Thirty_Thirty_Thrust()
Fire = Four_1.Avg()

pl.plot([53,109,136,182,246],[Seks,Ein,To,Tri,Fire]
        , "b--", label='Average Thrust')

#Plots the given X-values(53,109,136,182,246mm)
#and the imported maks values on the Y-axis.
Sicks_2 = Sicks.Z1_Thirty_Thirty_Thrust().Maks()

One_2 = One.Z1_Thirty_Thirty_Thrust().Maks()

Two_2 = Two.Z2_Thirty_Thirty_Thrust().Maks()

Three_2 = Three.Z2_Thirty_Thirty_Thrust().Maks()

Four_2 = Four.Z2_Thirty_Thirty_Thrust().Maks()



pl.plot([53,109,136,182,246],[Sicks_2,One_2,Two_2,Three_2,Four_2]
        ,"r--", label="Maximum Thrust")

#Plots the given X-values(53,109,136,182,246mm)
#and the imported min values on the Y-axis.
Sicks_3 = Sicks.Z1_Thirty_Thirty_Thrust().Min()

One_3 = One.Z1_Thirty_Thirty_Thrust().Min()
```

```
Two_3 = Two.Z2_Thirty_Thirty_Thrust().Min()

Three_3 = Three.Z2_Thirty_Thirty_Thrust().Min()

Four_3 = Four.Z2_Thirty_Thirty_Thrust().Min()

pl.plot([53,109,136,182,246],[Sicks_3,One_3,Two_3,Three_3,Four_3]
        ,"g--", label="Minimum Thrust")

#Plots the given X-values(53,109,136,182,246mm)
#and the imported Take-off values on the Y-axis.
Sicks_4 = Sicks.Z1_Thirty_Thirty_Thrust().Take_off()

One_4 = One.Z1_Thirty_Thirty_Thrust().Take_off()

Two_4 = Two.Z2_Thirty_Thirty_Thrust().Take_off()

Three_4 = Three.Z2_Thirty_Thirty_Thrust().Take_off()

Four_4 = Four.Z2_Thirty_Thirty_Thrust().Take_off()

pl.plot([53,109,136,182,246],[Sicks_4,One_4,Two_4,Three_4,Four_4]
        ,"y--", label="Take off thrust")

pl.ylabel("Effiency (N/W)")
pl.xlabel("Distance (mm)")
pl.title("Efficiency different distances. 30U 30L")
pl.show()
```

C RCbenchmark script

```
 /* ################ Thrust step up Coaxial ################
/\ Thrust
|                                                  _.  Max(99)
|                                              _./  \
|                                          _./      \
|                                      _./           \
|                                  _./                \
|                              _./                     \
|                          _./                          \
|                      _./                               \
|                  _./                                    \
|              _./                                        \
|          _./                                            \
|      _./                                                \
|   _./ Min(24N)
|_./ initESC
|_____________________________________________________> Time

############# Defined variables ############ */


var outputs = ["escA"];   // Setts Variable for Coxial propell A
var outputs1 = ["escB"];  // Setts variable for Coxial propell B
var step_up = [1200];     // Start point, throtel for Coxial propell B
var step_up1 = [1200];    // Start point, throtel for Coxial propell B
var minVal = [1300];       // Start point for ramping up A
var maxVal = [1300];       // Start point for ramping up B
var filePrefix = "28x28_Z0_test_1"; // Fil navn
var samplesAvg = 62;         // Data points from sensors
var diffrence = [1302];     // sluttpunktet for ramp up A & B
var Min = 24;               // Start testing at 24N
var Max = 100;               // End point testing 99N +1N
rcb.files.newLogFile({prefix: filePrefix}); //Creating file
//readSensor();
rcb.sensors.tareLoadCells(initESC); //Reseting loadcells

//Running Propeller A & B to start point.
function initESC(){
    rcb.console.print("Initializing ESC...");
    rcb.output.set(outputs, step_up1);
    rcb.output.set(outputs1, step_up);
    rcb.wait(Callback, 2);
}

// Records a sample to CSV file
function takeSample(callback){
    rcb.sensors.read(function (result){
        // Write the results and proceed to next step
        rcb.files.newLogEntry(result, callback);
    }, samplesAvg);
    // Steping value up 5N to next testing point
```

```
    Min++;
    Min++;
    Min++;
    Min++;
    Min++;
    //Checking if Thrust have exceded Max value
    if(Max > Min){
        rcb.wait(Callback, 4);
    }else{
        //Call for ending script
        rcb.wait(EndScript,4);
    }
    }

    //Ends script
    function EndScript(){
        rcb.endScript();
    }

    //Reading sensors to get thrust
    function Callback(){
        rcb.sensors.read(Correction);
    }

    // Ramping up propeller A & B, and checking if our system have reatched
    //the deciered thrust.
    function Correction(result){
        var thrust = result.thrustDual.displayValue;
        diffrence++;
        diffrence++;
        minVal++;
        minVal++;
        if(thrust < Min){
            var duration = 2;
            rcb.output.ramp(outputs1, minVal, diffrence, duration);
            rcb.output.ramp(outputs, minVal, diffrence, duration);
            rcb.wait(Callback, 2);
        }else{
            rcb.wait(takeSample, 2);

        }
    }
```